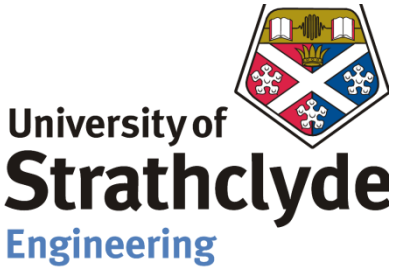

Department of Mechanical Engineering

Wind-Hydrogen Community on the Isle of Lewis

Author: Gordon Robertson

Supervisor: Dr Nick Kelly

A thesis submitted in partial fulfilment for the requirement of degree in

Master of Science in Energy Systems and the Environment

2009

Copyright Declaration

1. Abstract

An increasing number of islands around the world are turning to renewable power systems to generate the electricity they require so that they are less dependent on energy imports from the mainland. This helps to ensure more reliable electricity supply to the local community as well as reducing the higher costs associated with energy imports. This project investigates the potential of a wind-hydrogen system on the Scottish Outer Hebridean island of the Isle of Lewis.

The proposed area of Lewis where this wind-hydrogen system would be placed experiences frequent cuts in electricity since the community is at the end of the line of a weak electrical grid. If the installation of renewable energy systems such as wind farms are to be solely relied upon for energy, an energy storage medium (in this case, hydrogen) is required to solve the problems of intermittent energy supply from the wind farm.

This project uses wind data collected from a meteorological site on the West coast of Lewis to determine the energy output from a theoretical 2.73MW wind farm. Electrical demand data is generated for an average household in the community to determine the size of hydrogen system required to meet the primary project aim of supplying electricity to the community all year round.

Microsoft Excel has been used to simulate the wind-hydrogen system and to determine the number of households the 2.73MW wind farm could supply with their annual electricity requirements. In addition to this, the hydrogen fuel cells used in the system will act as mini-CHP units supplying the households with both power and heat through the use of a heat exchanger integrated into the fuel cell's cooling circuit and household's hot water system.

The efficiencies of the fuel cells and hydrogen producing electrolysers are obtained through practical experimentation with a 600W fuel cell to determine the units' performances under transient loading conditions.

2. Acknowledgements:

I would like to begin by saying thank-you to Dr Nick Kelly who was my project supervisor and provided me with the topic of research and gave me guidance throughout the duration of the project. Dr Kelly also set-up the initial contacts with Greenspace Research on the Isle of Lewis (Stornoway).

I would also like to acknowledge the help I was given during my stay in Stornoway by the team at Greenspace Research and the Lews Castle College staff, in particular, Dr Alasdair Macleod, Dr Neil Finlayson and Ms Sally Bell. Dr Macleod assisted me with some of the experiments carried out in the Lews Castle College hydrogen laboratory and Ms Sally Bell was responsible for my accommodation arrangements during my stay and a point of contact if any help was needed.

Acknowledgement also goes to the Western Isles council who, along with Greenspace Research, fronted half of the money for my accommodation and travel expenses to island. Rhuari MacIver from the council gave his valuable input to my project when discussing the best location for the wind farm to be used in the project.

Finally, I am grateful to Donald Mackenzie from Scottish & Southern Energy for his efforts in trying to obtain energy demand data for the chosen community in the project and Brian and Kath Griffiths, for the data they kindly supplied me with on annual heating demands for a typical household on the island.

Table of Contents

List of Tables & Figures:

3.1 Introduction:

There is an increasing demand for the development of renewable energy schemes in Europe and the United Kingdom (UK) to help cut CO_2 emissions and meet renewables targets set-out by the European Union (EU) for 2020. The Western Isles of Scotland have an abundance of renewable energy resource which could be used to meet the renewable energy targets both the UK Government and Scottish Executive have set for the future.

At the end of 2008, 5.5% (21,597 GWh) of the electricity generated in the UK was from renewable energy sources [1]. The UK government in April 2009 officially agreed to conform to the EU wide 2020 target for 20% of all Europe's energy to come from renewable sources [2]. The UK's contribution to the EU target will be for 15% of all energy generated from renewables. This is notably less than the contributions coming from other EU countries such as Sweden and Germany. To achieve this, it is proposed that 30% of the electricity produced, 12% of heating energy and 10% from transport will be produced from renewable sources [3].

The main problem with relying on renewable energy schemes such as wind farms for our energy is that their output is completely dependent on the available wind or energy resource. As such, their energy output at a certain time in the future cannot be accurately predicted which requires conventional fossil-fuel burning power stations to be available on stand-by. The UK National Grid has sufficient reserve capacity to cope with the intermittency of supply from the current renewables capacity connected to the grid. However, relying on renewables for 30% of the electricity as is proposed for 2020 will need additional power stations to act as a reserve [4].

Another problem the UK faces in integrating renewable power generation into the National Grid arises from the need to build renewable power 'stations' in remote areas of the country. Northern Scotland offers some of the best renewable energy resource in Europe, however, there is insufficient (and in some cases non-existent) electrical infrastructure located in these remote areas to distribute the energy they generate to the demand centres in the South of the country. Further to this, transmitting large levels of electricity over long distances from these remote areas of the country would result in greater power losses [5].

3.2 Aims and Objectives:

In this study, a relatively small scale 2.73MW wind farm located on the West coast of the Isle of Lewis will be looked at to determine what size of community the farm could theoretically supply with the domestic energy requirements (heating and electricity) all year round. Success for smaller scale systems like this can be used as demonstrations for larger potential projects on the mainland which would lead to greater financial investment in the technologies. Increased financial investment in renewable technologies will undoubtedly progress their performance and efficiency whilst driving down the costs as the market for them grows. Stand-alone wind-hydrogen schemes on islands are of particular use as it removes the islanders dependence on the main grid connection which can be of poorer quality as well as the higher costs associated with fuel for heating since it must be imported from the mainland.

For this report, the problems faced with intermittent supply from wind farms are to be solved with the use of an energy buffering system. When the wind farm is producing more energy than there is demand, the energy can be stored in the form of hydrogen. This is achieved through the electrolysis of water splitting it into hydrogen and oxygen and then storing the hydrogen under compression. When the energy output from the wind farm falls below that of the demand from the community, the hydrogen is consumed by a fuel cell producing electricity and heat as a by-product. A simple illustration of this process is shown below in *Figure 1* where the blue shaded area represents the energy stored as hydrogen and the yellow shaded area represents the energy produced by the fuel cell from the hydrogen storage;

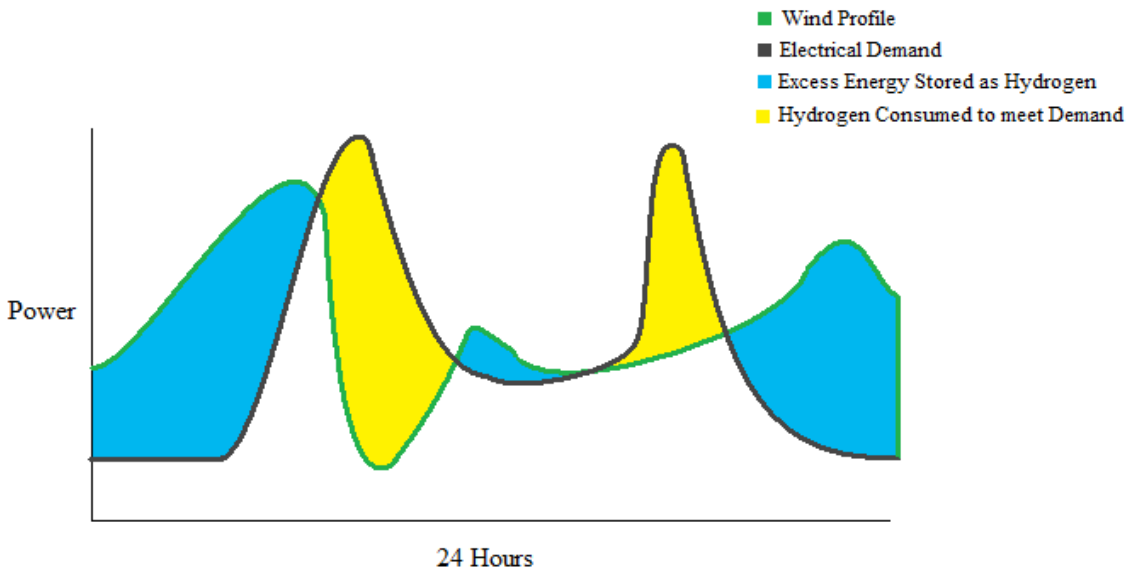

Figure 1 – Illustration of Hydrogen Energy Balance

To meet the objective of supplying the community with energy for space heating and domestic hot water, households were assumed to use a combination of heat recovery from the fuel cells as well as electricity from the wind farm in storage heaters and heat pumps to maximise the efficiency.

Wind data from the collected from the meteorological station at the proposed site for the wind farm on the Galson Estate (West coast of Lewis) was used to determine the annual energy output from the wind farm. In addition to this, Scottish and Southern Energy supplied the energy demands for the West coast of Lewis allowing for a more accurate energy balance of the wind-hydrogen system.

The electrical and thermal efficiencies of the fuel cell and electrolyser components in the wind-hydrogen system were generated from experimental results carried out in a hydrogen lab with Greenspace Research (Lews Castle College) on the Isle of Lewis. Microsoft Excel was then used to simulate the system using the data collected from the experiments, Galson Estate and Scottish & Southern Energy.

A simple representation of a hydrogen buffering system can be seen in *Figure 2* below;

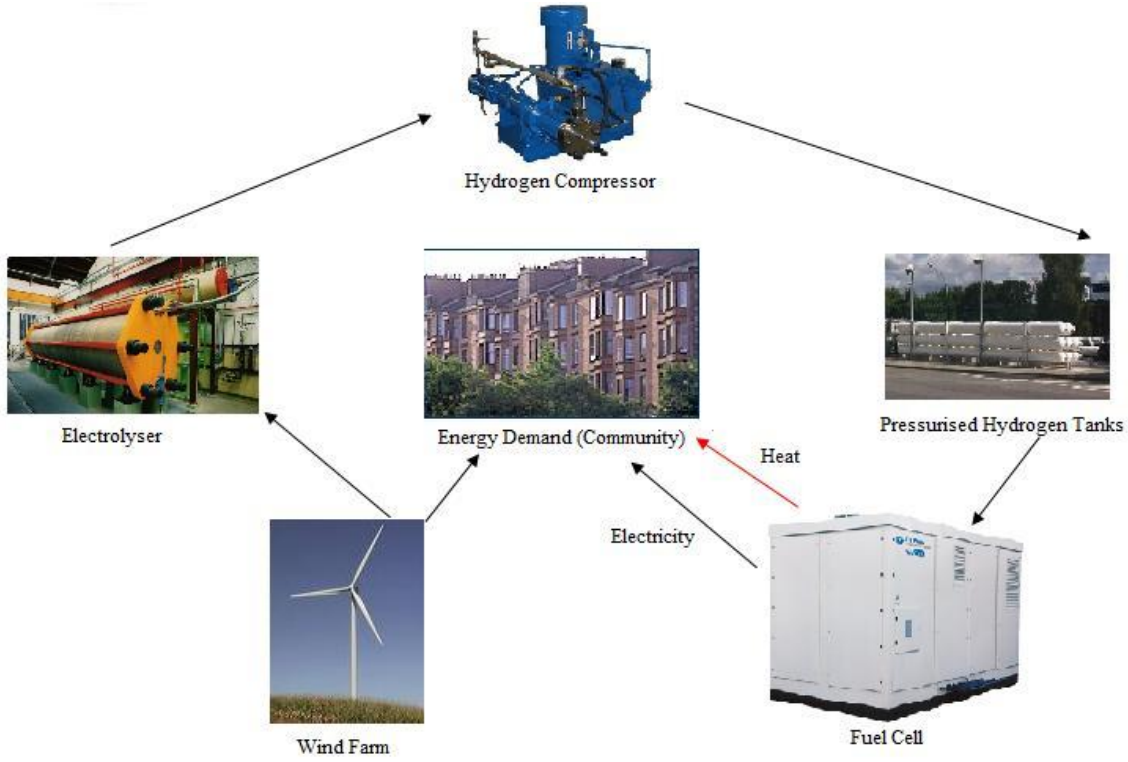

Figure 2 - Simple Representation of a Wind-Hydrogen System

4. Project Background:

4.1 Literature Review:

As has already been discussed, this project aims to investigate the technical feasibility of introducing a wind hydrogen scheme to the Isle of Lewis. The advantage of first looking at a relatively small wind farm on the island is that the system can be easily scaled-up to the incorporate a larger number of households on Lewis.

There are several wind-hydrogen projects in existence (particularly on islands) that are of a smaller scale than is proposed in this project. Four of such projects have been studied in this literature review and a brief summary of each is presented in the following section, each designed to serve slightly different purposes.

4.1.1. Utsira Project:

Utsira is a small island of around 6km^2 in area located off the West coast of Norway. A company called Norsk-Hydro installed a wind-hydrogen scheme on the island to meet some of the energy demands of the local community which consists of approximately 235 inhabitants [6]. The peak power demand from the island peaked around 900kW in 2006 with an average energy consumption over the year of 3.5GWh.

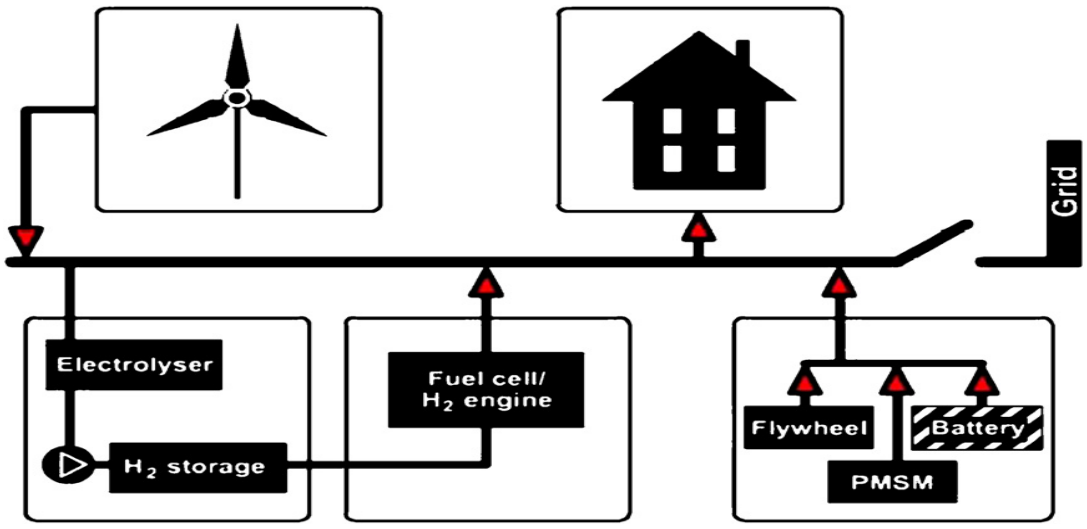

Figure 3 - Utsira Wind-Hydrogen System [7]

The wind-hydrogen project built by Hydro is the world's first full scale system of its kind supplying all of the energy needs of 10 households on the island as well as delivering energy to the rest of the island when there is sufficient wind resource. The project was completed and operational by the summer of 2004. The project consists of two 600kW wind turbines built by the German manufacturer, Enercon. These turbines deliver energy to the local island grid as well as a hydrogen station located at the base of the turbines when there is excess wind energy available.

The hybrid hydrogen station uses two forms of energy storage. The first is in the form of hydrogen gas using a 48kW electrolyser capable of producing $10Nm^3/h$ of hydrogen gas, and the second is a mechanical flywheel capable of storing 5kW in its rotating mass which is used as a buffer to supply a stable power supply to the grid from the variable output wind source. Within the hydrogen station, there is also a 10kW fuel cell from a small Danish company IRD and a 55kW hydrogen internal combustion engine (HICE) which supply the energy needs to the 10 households when there is insufficient energy produced from the turbines. The hydrogen storage tank has a capacity of $2400Nm^3$ which should have an energy content of approximately 7200kWh.

The future goal for the project is to make the island fully grid independent using local renewable energy resource and possible export excess energy produced back to the mainland.

4.1.2. PURE Project:

The PURE (Promoting Unst Renewable Energy) project is the world's first community owned renewable hydrogen scheme. Unst is the most northerly island in the UK located in the Shetlands. The island has a population of 500 and a larger area of land when compared to Utsira of $60miles^2$.

The project was designed and by PURE, The Unst Partnership Ltd (local Government), siGEN (Fuel cell manufacturers) and the Robert Gordon Engineering faculty in Aberdeen on a budget of £350,000 [8].

Figure 4 - PURE Project (Unst-Shetland Islands) [8]

The project uses two commercial prototype 15kW wind turbines as the primary energy source for the scheme as wind turbines were the most economically viable. They found that there was a lack in the wind turbine market for commercially available wind turbines in the rated power region of 6-300kW. Additionally, it was found that smaller scale community sized turbines lacked active yaw and pitch control which aid in operating efficiency of the turbines. As such, the PURE project team were involved in the development of the 15kW turbines eventually used.

Despite the system using wind turbines as the primary energy source, it was designed so that it could use any other energy source which would cater for future expansion of the scheme. The main aims of the system were to supply heat to five businesses on the island as well as hydrogen for a fuel cell vehicle and a back-up fuel cell.

Excess wind energy is used to supply a high pressure electrolyser capable of producing 3.55Nm^3/h of hydrogen which is then stored in pressurised gas cylinders ready to be used either at the filling station for the hybrid vehicle or in the back-up fuel cell. The back-up fuel cell supplied by siGEN is rated at 5kW and is used to deliver electricity to the 5 businesses when there is insufficient wind.

The unregulated AC output from the wind turbines is fed through AC-DC rectifiers before being used in storage heaters in the heating load. The PURE project designers thought the best use of the wind turbines energy would be to supply heat rather than power. This has the advantage of naturally matching energy supply with demand as there is a correlation between high wind speeds and the thermal energy lost from buildings as a result. Therefore the energy captured by the turbines during the high wind speeds is used to replace the energy lost from the buildings.

4.1.3. Lolland Project:

Lolland is an island in Denmark where a demonstration project for a hydrogen community is being developed. The project has been split into 3 phases. At present, phase 1 is complete and work on phase 2 is under way. The island has an abundance of wind resource from off-shore wind turbines, however, the majority of the energy is generated at night times when the instantaneous demand for it is at its lowest. As such, the need for an energy storage system is required if the island is to be self sufficient on renewable energy.

Phase 1 began in 2007 making use if the excess energy from the turbines to generate hydrogen through the electrolysis of water [9]. 10 households were fitted with fuel cells from IRD which were used as combined heat and power (CHP) systems in a micro-generation scheme. Hydrogen is piped to these CHP systems from a centralised electrolyser, compressor and hydrogen storage station. A diagrammatic representation of the system can be seen below in *Figure 5*.

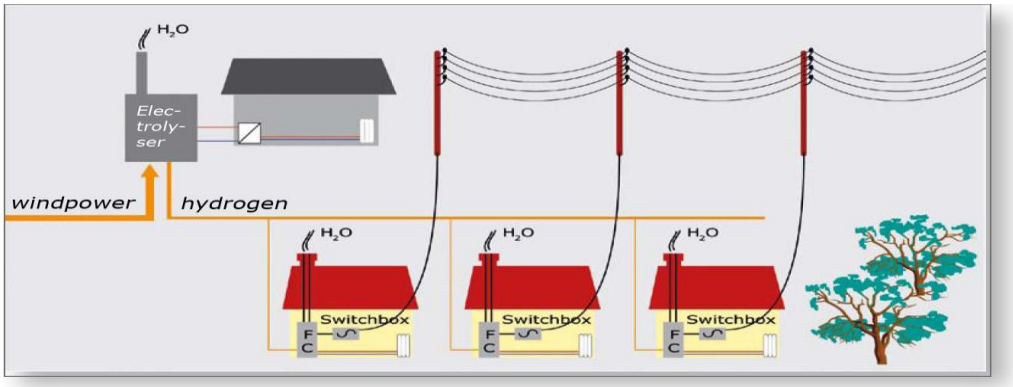

Figure 5 - Lolland Demonstration [10]

The project uses two 4kW electrolysers from the Canadian company, Hydrogenics which produces hydrogen gas to be stored under compression (6 bar) in a 50Nm^3 capacity tank. Each house is to be fitted with a 2kW Proton Exchange Membrane (PEM) fuel cell which supplies it with the heat and power needs.

Future plans for the project are to expand to supply 35 households on Lolland and 100 households nationally in phase 2.

4.1.4. HARI Project (UK):

The HARI (Hydrogen And Renewables Integration) project (2001-present) is based in West Beacon Farm (Leicestershire, UK) where hydrogen is being used in combination with renewable power generation to balance the energy supply and demand. There are small scale wind turbines, photovoltaic panels and micro-hydroelectric energy generators on site supplying the domestic and business buildings [11].

The project focussed on introducing a hydrogen energy system to the existing renewable power systems in place on the farm. These systems included; two 25kW wind turbines, 13kW photovoltaic installation, two micro-hydroelectric generators with a combined rating of 3kW. In addition to the renewables, a 10kW ground source heat pump is used for domestic heating purposes and an LPG (Liquid Petroleum Gas) fuelled CHP unit producing 15kW of electrical power and 38kW of thermal energy. Other sustainable technologies that are in place which make use of passive solar heating and collection of rainwater for domestic uses (as well as the electrolyser in the HARI project) due to the lack of a mains water supply.

The HARI project introduced a hydrogen energy storage (HES) system to the farm which replaced 120kWh capacity of lead acid batteries which had been used to balance energy supply and demand in combination with the electrical grid. The HES system used a 36kW alkaline electrolyser from Stuart Energy Europe company which produced hydrogen gas at a pressure of 25 bar. The claimed maximum efficiency for this electrolyser is 3.9kWh/Nm^3. This roughly equates to a stack efficiency of 75% which is higher than most electrolysers achieve in practice.

The hydrogen produced by the electrolyser is stored as a compressed gas as in the other projects looked at previously in this thesis (compressed gas storage is the cheapest solution, particularly as stationary storage doesn't have the same design constraints for space) however, more expensive but compact hydride storage is to be looked at in the future. The project uses 48 steel gas cylinders each with a volume of 0.475m^3 compressed to 137 bar giving an actual storage volume of 2856Nm^3. This gives the farm an energy storage capacity of 3.8MWh running through the fuel cells which is enough to run the farm for 3 weeks with no other energy input. A diaphragm type gas compressor is used to raise the electrolyser exit gas pressure up to 137 bar for storage in the cylinders. A small buffer tank is used with the compressor to ensure a steady gas supply rate to the compressor which can be seen in the figure below (*Figure 6*). In addition to the hydrogen storage, the project makes use of a 20kWh battery for short term energy storage when the there is surplus energy from the renewable energy systems that the electrolyser can't absorb.

Figure 6 - HARI Diaphragm Compressor and Buffer Tank [11]

West Beacon Farm has two PEM fuel cells installed used to supply both heat and power to the project. The smaller of the two fuel cells is a 2kW CHP unit which produces $2kW_{elec}$ and $2kW_{thermal}$ at peak loading. The heat from the fuel cell is recovered from the cooling circuit and passed through a heat exchanger linked into the building's central heating system. The larger of the two fuel cells is set up to produce power only at present for the farm. It is a 5kW unit developed by siGEN and there are plans to convert this unit into a CHP device as well.

These four demonstration projects have all been developed over the past 9 years and each have been used for slightly different purposes. It is proposed that the techniques learnt from these projects are used in the hypothetical wind-hydrogen project on the Isle of Lewis and scaled-up to meet the higher energy demands. In the following section, details of the components used in wind-hydrogen projects will be outlined for the reader.

4.2 Wind-Hydrogen Components:

4.2.1. Wind Turbines:

The most common type of wind turbine used for large scale power generation is the three bladed horizontal axis wind turbine (HAWT). Before the wind was used to produce electricity, windmills have been used for mechanical work such as grinding grain and pumping water for centuries. The first windmill built for the production of electricity was in Scotland in July 1887 by Professor James Blyth of what is now known as Strathclyde University [12]. The windmill was used to provide power for the lighting in his house. Later, in the 1890s, Danish scientist, Poul La Cour developed wind turbines which were used to produce hydrogen from water.

With the increasing demand for electricity at the beginning of the twentieth century and the strain on fuel resources caused by the war, windmills were converted to generate electricity rather than be used for more traditional purposes. However, serious development of wind turbines for electrical power output didn't begin until the oil crisis in 1973 where energy producers sought alternative means of producing energy without relying on finite resources of fossil fuel [13].

Figure 7 - E44 Enercon Wind Turbine

The image shown above in *Figure 7* is of an Enercon E44 wind turbine with a rated power of 910kW and a peak power coefficient of approximately 0.5. The turbine uses a direct drive, synchronous generator to produce electricity. This is the turbine that is proposed for the small wind farm in this project on the Galson estate (Isle of Lewis).

The Enercon E44 turbine operates between wind speeds of 3m/s and 25m/s (with a storm control system that allows brief gusts up to much higher wind speeds without damaging the turbine or generator). The turbine power output increases with the wind speed up to its rated design wind speed of 15m/s where the onboard control systems pitch the individual blades accordingly so as not to overload the generator.

Wind turbines are always kept facing directly into the wind when they are in operation so as to capture as much energy as possible. This is achieved on larger turbines such the ones being used in this project via yaw control system connected to electric motors inside the turbine. A wind vane sits on top of the nacelle sending information about the wind direction to the yaw control system so that the blades are always kept facing into the wind. On smaller and lighter systems, a vertical stabiliser is often used that to naturally keep the blades pointing into the wind. A simple diagram of the components found inside a wind turbine is shown below in *Figure 8*;

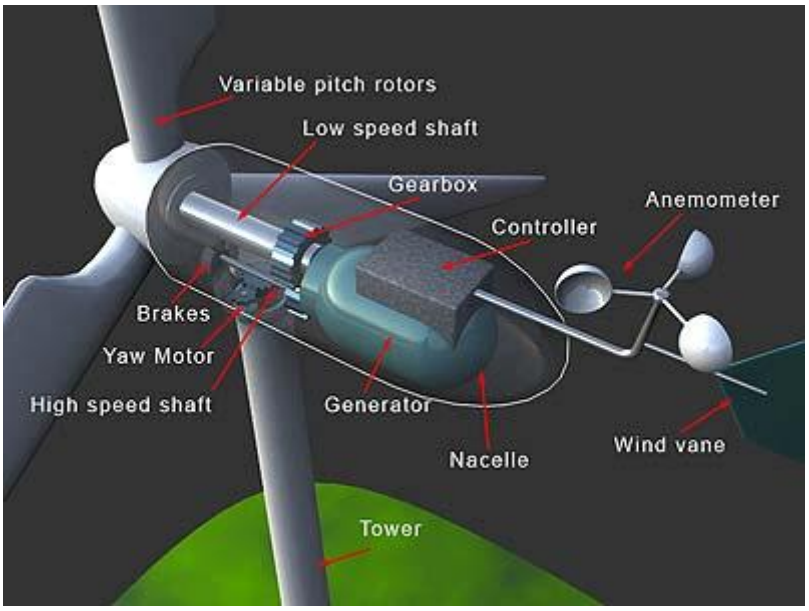

Figure 8 - Wind turbine components

It is worth noting that not all wind turbines have the same components as shown in the diagram above. This depends for instance on whether the generator is a direct drive system, (large diameter generators with many poles which therefore require a low speed input negating the requirement of a gearbox) or as shown above, driven through a gearbox which is needed to increase the low rotational speed of the wind turbine (typically between 20 and 50 rpm) up to 1000 to 3000 rpm.

The pitching control mechanism seen on the blades of the wind turbine is used to maximise the wind turbine efficiency as the wind speeds pick up to rated. At rated speed the blades are pitched to keep the rotational speed of the blades constant as mentioned above. The pitching mechanism is also used to bring the turbine to a stop when the wind speeds get to high or for shutdown during maintenance intervals. In addition to this aerodynamic braking system, the turbine shaft also has a large hydraulic disc brake which could be used in emergency shutdown procedures and to hold the blades stationary when the wind turbine is inoperative. Having pitched controlled blades (as opposed to fixed speed turbines) on larger wind turbines (~1MW plus) also reduces mechanical stresses on the turbine as they can absorb sudden gusts of wind in the mechanical inertia of the turbine which reduces the torque pulsations. Removing some of the torque pulsations also allows the generator to deliver better power quality as fluctuations such as 'flicker' are reduced

Wind Turbine Generator Types:

Most large wind turbines of the size being used in this project and above use doubly-fed induction type generators, however, an increasing number of direct drive synchronous generators are being introduced in the large wind turbine market. German wind turbine developers typically favour the latter type of generators as is used in the Enercon E44 wind turbine which has a direct –drive multi-pole synchronous generator.

Induction generators are widely used as they are generally cheaper than synchronous machines, they are durable and if there is a fault in the grid network then the turbines will shut-down. Induction machines can operate in sub or super-synchronous conditions. These conditions refer to the rotor speed relative to the synchronous speed of the machine (this is

known as ‘slip’). In super-synchronous mode, the machine operates as a generator where current is delivered from the rotor, through the converters (which de-couple the generator speed from the grid frequency) to the grid. When the rotor inside the induction machine is rotating slower than the designed synchronous speed, power is absorbed from the grid and the wind turbine essentially becomes large fan with the induction machine acting as a motor. These types of generators therefore must absorb some reactive power from the grid to magnetise the stator until the torque supplied from the wind turbine is sufficient to achieve the super-synchronous condition. A diagram of slip conditions can be seen in *Figure 9* below.

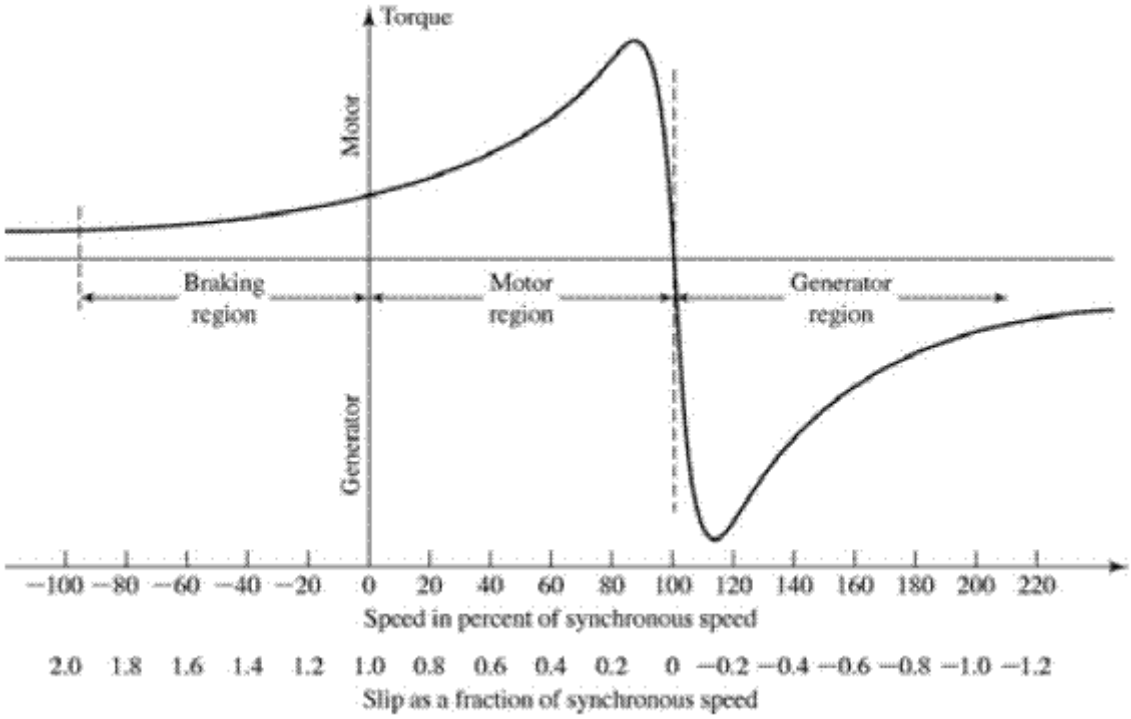

Figure 9 - Induction Machines Slip Condition

Synchronous generators can be connected to the wind turbine directly or indirectly through a gearbox. Direct drive generators tend to be large in diameter with multiple poles whereas the use of the gearbox allows for fewer poles in the generator and thus a smaller diameter. Additionally, the generators can use electrically excited magnets (electromagnets) or permanent magnets. As before, the generator is de-coupled from the grid with the use of a power converter. The power converter arrangement can either consist of a diode rectifier on

the generator side to convert the AC output to DC before a pulse width modulated voltage source converter (PWM VSC) converts the DC to the AC grid frequency, or use two PWM VCS on both sides of the converter.

Maximum Power Coefficient:

The power coefficient refers to the amount of energy the wind turbine can extract from the airflow through the rotor disc. In the case of the Enercon E44 and most larger scale HAWTs, a peak of 50% of the available energy in the wind is extracted by the turbine. The theoretical maximum is known as the Betz limit where momentum and actuator disc theory are used to calculate the limit. *Figure 10* below illustrates a 2-D representation of a stream tube around a rotor disc.

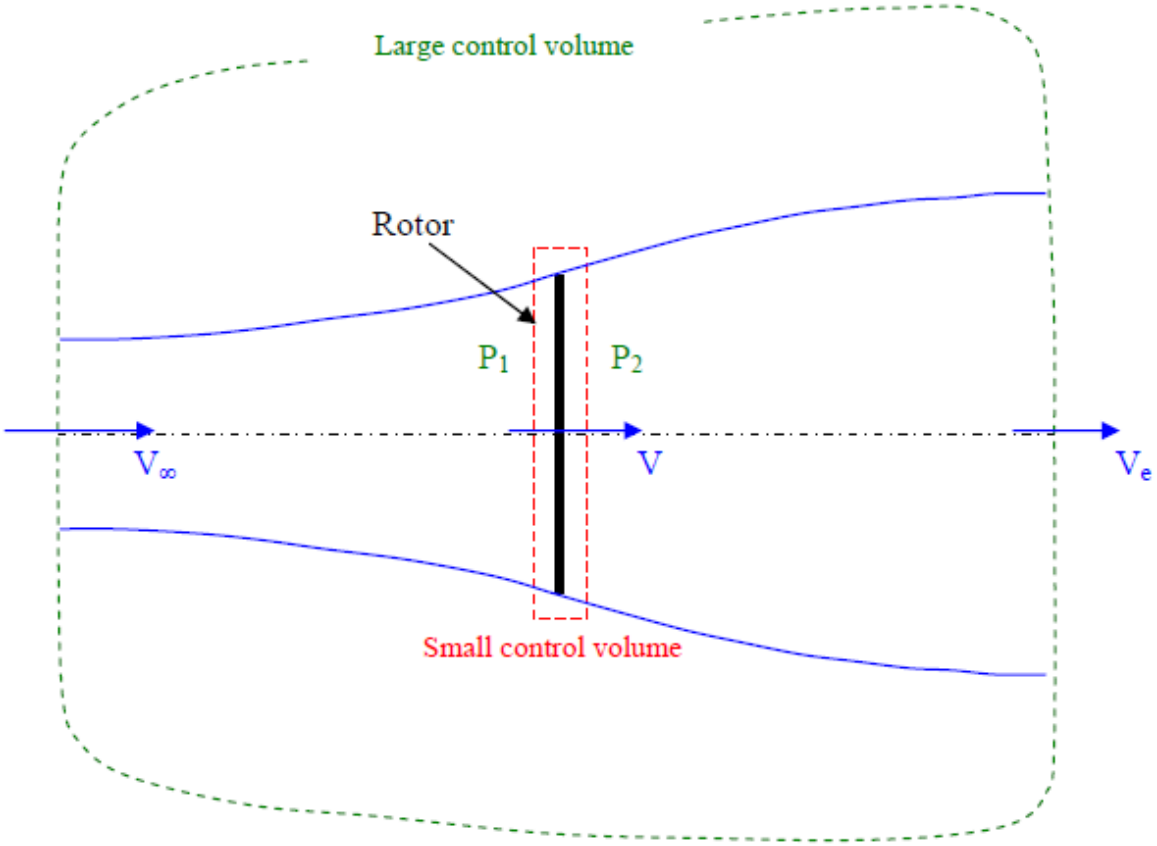

Figure 10 - Stream Tube for 2D Rotor Disc [15]

As can be seen in the figure above, the stream tube far upstream from the rotor is of a smaller diameter than the rotor itself. The presence of the rotor in the tube causes the incoming air to slow down as it approaches it resulting in the expansion of the stream tube. Since no work has been done on or by the air at this point, the static pressure rises above atmospheric pressure to account for the decrease in kinetic energy in the flow [14]. When the air crosses the rotor, the wake pressure drops below atmospheric levels found outside of the stream tube before eventually returning to atmospheric pressure further downstream of the rotor. The return to this equilibrium pressure is again at the expense of kinetic energy in the wind thus reducing the flow speed further. The difference in the kinetic energy of the flow upstream of the stream tube and far downstream is the energy absorbed by the wind turbine.

The Betz limit can be calculated from the following equations. The mass flow rate of the wind is determined by the air density, ρ, the cross sectional area of the disc, A and the flow velocity, V. The mass flow rate is the same at all points through the stream tube, however, the disc induces an inflow velocity to the free stream velocity known as an inflow factor, a. The inflow factor is given by the equation;

$$V_{disc} = V_{\infty}(1 - a) \qquad (1)$$

From momentum theory, the change in momentum from the far upstream velocity to the far downstream velocity can be calculated from;

$$Rate\ Change\ of\ Momentum = (V_{\infty} - V_e)\rho A V_{disc} \qquad (2)$$

The expression for the power extracted from the wind by the rotor is given by;

$$P = \frac{1}{2}\rho A V_{disc}\,(V_{\infty}^2 - V_e^2) \qquad (3)$$

Equation 2 can be re-arranged to give equation 4 which can be substituted into equation 1 to give equation 5 as follows;

$$V_{disc} = \frac{1}{2}(V_{\infty} - V_e) \qquad (4)$$

$$V_e = V_{\infty}(1 - 2a) \qquad (5)$$

Substituting equation 5 into equation 3 now gives a new expression for the power extracted by the wind turbine which can be differentiated to obtain a value for the inflow factor, a, at maximum and minimum power ratings;

$$P = 2\rho A V_{\infty}^3 (a - 2a^2 + a^3) \qquad (6)$$

Differentiating the power with respect to the inflow factor, then factorising the solution gives two stationary points on the power curve relating to maximum and minimum power. It is found that maximum power is obtained at an inflow factor of a third. Using this value in the power equation and then substituting the solution into the equation for maximum power coefficient gives the following solution to the Betz limit;

$$C_{P_{max}} = \frac{\frac{8}{27}\rho A V_{\infty}^3}{\frac{1}{2}\rho A V_{\infty}^3} = \frac{16}{27} = 0.593 \qquad (7)$$

Where the numerator in equation 7 represents the solution for maximum power extracted by the rotor and the denominator is the maximum energy available in the wind flow. The Betz limit states that the theoretical maximum power coefficient for a wind turbine is 59.3%.

However, this equation does not take into account energy found in tip vortices or the rotational velocity component in the wake. As such, real turbines which have been efficiently designed are expected to achieve lower maximum power coefficients of around 50%.

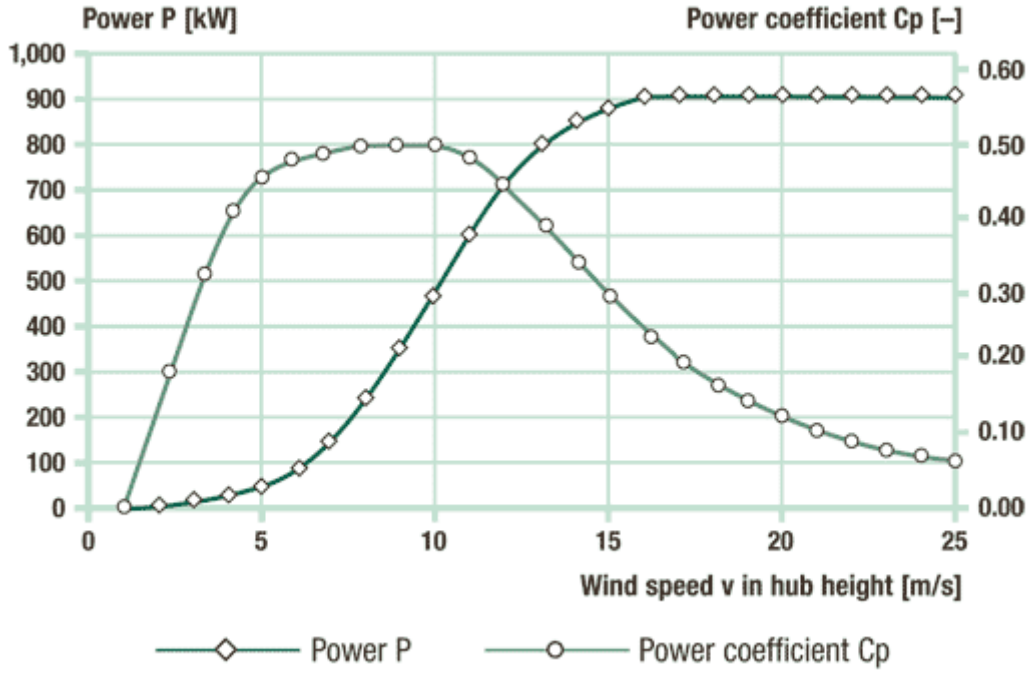

Figure 11 - Power and Cp curves for Enercon E44 Turbine

Figure 11 above illustrates the power curve for the wind turbine to be used in this project as well as the power coefficient. This graph highlights the above point made with regards to the theoretical maximum power coefficient being higher than the actual value.

4.2.2. Fuel Cells:

The method of generating electricity through the use of a hydrogen fuel cell is both sustainable and completely clean since the only emissions from the process are air and water vapour. A fuel cell also has a very simple method of operation which uses no moving parts (apart from ancillary devices such as pumps and fans). However, the main problem with using hydrogen as the fuel is that despite there being an essentially limitless supply of it, pure hydrogen is not readily available and energy is required to extract it (see later section on electrolysers).

The first fuel cell reaction was produced in 1839 by scientist and lawyer, William Grove [18]. This involved a simple reaction using a liquid acid electrolyte and two platinum electrodes connected by a circuit to produce a DC current. Since fuel cells produce DC current and household mains power supply is AC, power conditioning in the form of an inverter must be used in this project.

There are six main types of fuel cell. The different fuel cells are defined by the type of electrolyte used as well as fuel source among other factors. These types are; Alkaline, Proton Exchange Membrane, Direct Methanol, Phosphoric Acid, Molten Carbonate and Solid Oxide fuel cell. The table below highlights some of the properties of these fuel cells;

Fuel Cell Type	Mobile Ion	Operating Temp (^{o}C)	Applications
Alkaline (AFC)	OH^-	50-200	Spacecraft
Proton Exchange Membrane (PEMFC)	H^+	30-100	Vehicles, lower power CHP
Direct Methanol (DMFC)	H^+	20-90	Portable low power systems
Phosphoric Acid (PAFC)	H^+	~220	Medium power CHP systems
Molten Carbonate (MCFC)	CO_3^{2-}	~650	Medium to large scale CHP

Solid Oxide (SOFC)	O^{2-}	500-1000	Low to large scale CHP systems

Table 1 - Fuel Cell Properties [18]

The diagram below (*Figure 12*) illustrates the reaction process inside a PEMFC;

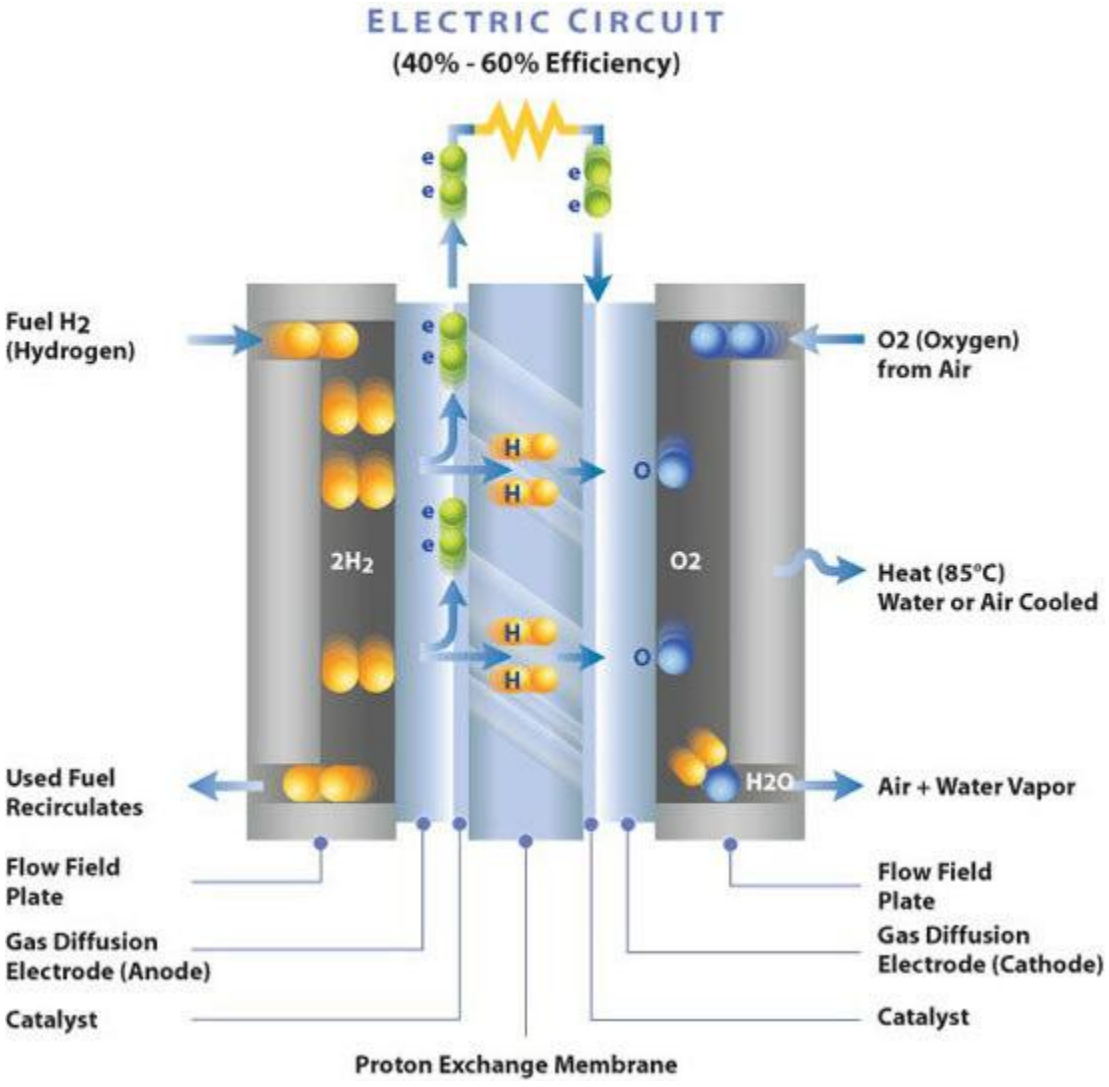

Figure 12- Proton Exchange Membrane Fuel Cell [19]

The PEMFC (which is used in this project) uses a solid polymer electrolyte which only allows protons to pass through thus forcing the electrons through an external circuit. The chemical reactions which occur at both of electrodes are shown below;

$$Anode: \quad 2H_2 \rightarrow 4H^+ + 4e^- \qquad (8)$$

$$Cathode: \quad O_2 + 4e^- + 4H^+ \rightarrow 2H_2O \qquad (9)$$

Hydrogen gas is supplied to the anode electrode where the platinum catalyst works to ionise the hydrogen. Ionising the hydrogen gas molecule releases 4 hydrogen ions (4 protons) and 4 electrons as shown in equation 8 above. Since the solid polymer electrolyte only allows the protons to pass through the middle of the fuel cell, the electrons are forced to pass through the external circuit creating an electrical current. The positively charged protons are drawn through the electrolyte to the negatively charged cathode where they recombine with the electrons and the oxygen in the air being pumped over the cathode to form water vapour as described in equation 9.

Due to the relatively low operating temperatures of a PEMFC when compared to some of the other types, the rate of the reaction can be quite slow. In order to speed up the reaction, porous electrodes containing the catalyst, platinum, are used to increase the surface area and speed up the rate of reaction. The advantage of the low operating temperature makes the fuel cell well suited to mobile applications since it has a very quick start-up period and energy is not consumed pre-heating the fuel as it is in higher temperature fuel cell types. It also makes the fuel cell suitable for use in residential micro-CHP systems; again, due to the start stop nature of operation and quick responses.

Since PEMFC require high purity hydrogen gas as a fuel, there use depends on there being sufficient supply of hydrogen which needs to be extracted from other sources such as water or natural gas. One solution is to use methanol as the fuel rather than pure hydrogen gas. DMFCs consume liquid methanol which presents better storage solutions when compared to PEMFC and the hydrogen doesn't need to be extracted from the fuel before use. The

disadvantage is that these types of fuel cells have low power outputs and are not really suitable for the type of application being looked at in this project.

Alkaline fuel cells have been extensively used by NASA for the past 50 years in their Apollo missions and in the current re-useable shuttle to supply the onboard electricity and drinking water. These fuel cells also use porous platinum coated electrodes like the PEMFC to increase the rate of reaction. Some systems have been designed to operate under high pressures which run at higher temperatures. The problem with the AFC is that the cathode requires a carbon dioxide free air supply so as not to poison the catalyst. As such, a pure supply of oxygen needs to be used to get round this problem

The phosphoric acid fuel cell operates at higher temperatures (see table 1) than the three already looked at which makes it more suitable for CHP systems. Using a fuel cell for both heat and power clearly increases the overall system efficiency. The drawback of the PAFC is that it obtains its hydrogen from a finite fuel source, methane, through an energy intensive process of steam methane reforming. As such, the methane reforming system considerably adds to the cost of the fuel cell despite its widespread use to date.

The high operating temperatures of the solid oxide fuel cell mean that they don't require expensive catalysts to increase the rate of the reaction due to the high energy environment. Additionally, natural gas is used as the fuel which is reformed inside the unit negating the requirement for a separate fuel reformer. The very high operating temperatures ($1000^{o}C$) do bring other problems though. Complicated and expensive ceramic materials are needed to cope with the extreme temperatures which add to the cost of the system. Additionally, more energy is consumed in the ancillary devices to pre-heat the air and fuel as well as the complex cooling system needed.

The final fuel cell type is the molten carbonate fuel cell. This is another high temperature fuel cell which means that it only needs a cheap nickel catalyst to achieve a good rate of reaction. Unlike the alkaline fuel cell, the MCFC relies on an air supply to the cathode containing carbon dioxide. The disadvantage of this fuel cell is that the electrolyte is a molten mix of corrosive lithium, potassium and sodium carbonates [18].

Fuel Cell Efficiency:

The maximum thermal efficiency of single cycle systems which rely on the combustion of a fuel in air is approximately only 30%. A major advantage of the fuel cell is that they can operate at efficiencies as high as 70%. The theoretical maximum efficiency of a single fuel cell can be calculated from the equation 10 below;

$$E = \frac{-\Delta h_f}{2Ne} \qquad (10)$$

Where E represents the EMF output of the fuel cell, h_f is the enthalpy of formation (hydrogen), N is Avogadro's number (the number of electrons in a mole of an element) and e is the charge on one electron. Depending on which heating value of hydrogen (enthalpy of formation) is used, the solution to equation 10 will differ accordingly. If the higher heating value of hydrogen gas is used (energy released condensing water vapour to a liquid, -285.84kJ/mol^{-1}), then the EMF of the cell is 1.45V. However, using the lower heating value (energy released burning hydrogen, -241.83kJ/mol^{-1}), the EMF will be slightly lower at 1.25V per cell. These voltages are what would be achieved if the fuel cell was 100% efficient. Since the voltage output from an individual cell is very low, in practice, many cells are connected in series to form a 'stack' raising the power output to the desired level. The cells in the stack are separated by bi-polar plates which have alternate channels on either side of the plate to separate the hydrogen and air supplies to the fuel cell.

In reality, fuel cells cannot convert all of the energy stored in the hydrogen into electricity as some of it is lost as heat during the reactions (assuming no hydrogen can leak from the system). A fuel cell operates at its highest electrical efficiency during minimum loads (opposite to internal combustion engines) and then decreases as the load is increased normally levelling out between 40% and 60% efficiency. Therefore, the actual fuel cell efficiency is calculated from;

$$\eta_{Fuel\ Cell} = \mu_f \frac{V_{actual}}{E_{LHV}} \qquad (11)$$

Where V_{actual} is the average measured individual cell voltage, E_{LHV} is the lower heating value EMF output at 100% efficiency calculated from equation 10 and μ_f is the fuel utilisation coefficient. The fuel utilisation coefficient refers to mass of fuel reacted in the cell over the mass of fuel supplied to the cell. This figure can be estimated between 0.95 and 0.98 to give a figure for the actual fuel cell efficiency.

4.2.3. Electrolysers:

An electrolyser can be thought of as the reverse process of a fuel cell since energy is consumed (DC electrical current) by the system in order to produce the hydrogen (the energy storage medium) to be used by the fuel cell when the energy is required.

As with the fuel cell, there are differing types of electrolyser based on the electrolyte that they use. These are; the alkaline electrolyser, the proton exchange membrane electrolyser and the solid oxide type.

The alkaline electrolyser is the most common type in use today, particularly in larger scale applications like fuel filling station forecourts. When compared to proton exchange membrane electrolysers, the alkaline type is cheaper due to the formers requirement for the expensive platinum catalyst. These electrolysers use a circulating alkaline liquid electrolyte (potassium hydroxide, KOH^-) to produce hydrogen gas at the cathode and oxygen gas at the anode in the chemical reaction shown below;

$$Cathode: \quad 2H_2O + 2e^- \rightarrow H_2 + 2OH^- \qquad (12)$$

$$Anode: \quad 2OH^- \rightarrow \frac{1}{2}O_2 + 2H_2O + 2e^- \qquad (13)$$

High purity hydrogen and oxygen are produced from this reaction (>99.8% and 99.2% respectively) at electrical efficiencies between 60% and 90% using the higher heating value (HHV). The higher heating value can be applied for electrolysers since this value relates to the enthalpy of formation of water and not steam. The electrolysers often operate under pressurisation which decreases the energy required for compression in a separate unit post electrolysis [20]. However, the alkaline electrolyte is very corrosive to the electrodes when the input current is stopped. As a result, the electrolyser needs to have a continuous power supply between 10% and 40% of the peak loading to maintain polarisation of the electrodes [22]. The water being supplied to the electrolyser needs to be fed through a purifier before entering the stack. The diagram below in *Figure 13* illustrates the components needed for an alkaline electrolyser;

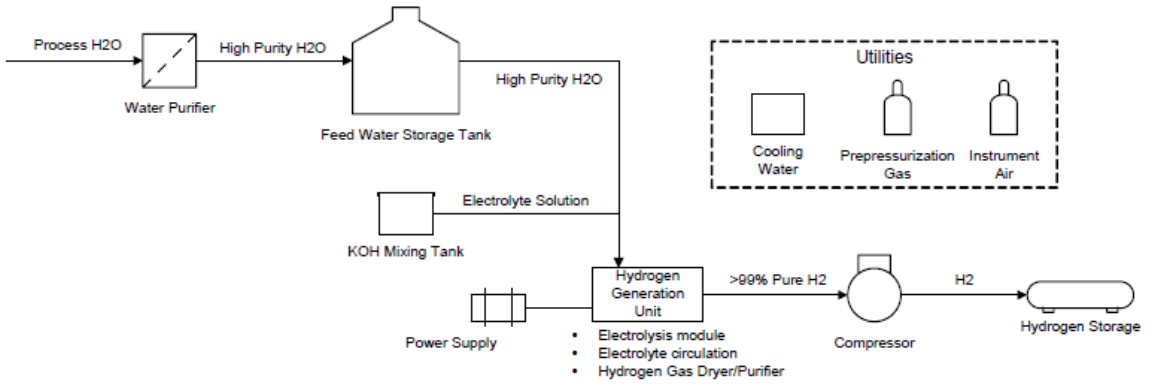

Figure 13 - Alkaline Electrolyser Systems [21]

The PEM electrolyser uses the same solid polymer electrolyte as the PEM fuel cell, Nafion, which is a fluorocarbon based ionomer. As such, the chemical reaction which occurs inside the stack is the reverse of equations 8 and 9 (see previous fuel cells section on PEMFC). The PEM electrolyser has proven reliability operating under real world environments continuously for over 100,000 hours. Higher purity hydrogen is achieved when compared to alkaline electrolysers of 99.999% and higher current densities (more compact unit) at efficiencies between 50-90% (HHV). Efficiency is lost in the PEM electrolyser like the PEMFC when operating under higher current densities. The advantage of the PEM electrolyser is its ability to operate under transient current supplies as would be experienced by the electrolyser being used in this project.

Like the SOFC, the solid oxide electrolyser operates at very high temperatures requiring inexpensive catalyst material on the electrodes. However, the same problems exist in manufacturing and handling the ceramic materials as well as achieving comparable operating lives when compared to the other two types of electrolyser [20].

4.2.4. Hydrogen Properties:

Hydrogen is the most abundant element in the universe and is present in all manner of substances on earth. Hydrogen is the simplest and lightest element in the periodic table containing only one proton and one electron. Some radioactive isotopes of hydrogen contain neutrons such as deuterium and tritium. The chemical arrangement of a hydrogen atom is very reactive which means hydrogen atoms will readily combine with other atoms meaning it doesn't occur naturally on its own and must be separated from the other atoms before use (see section on electrolysers).

Hydrogen is a gas at room temperature and has the second lowest boiling points of all the elements at -253^{o}C and is a solid at -259^{o}C (only 14 degrees Kelvin above absolute zero). This makes hydrogen a cryogenic substance when in solid or liquid state. At room temperature therefore, hydrogen is a colourless, odourless and tasteless gas which is non-toxic to humans (unless in an enclosed space where the volume of the gas displaces too much oxygen which would result in asphyxiation) [24].

With the hydrogen atom being the simplest of all elements, it has the lowest atomic mass. This means that the density of the hydrogen is very low when compared to other elements and fuels. For instance, under standard atmospheric conditions, hydrogen gas at 1 bar of pressure has a density of 0.0899kg/m^3, whereas petrol is a liquid under standard conditions with a density of 700kg/m^3. Even using an energy intensive process to cool hydrogen into a liquid still results in a very low density of 70kg/m^3. This can be illustrated by the fact that a cubic meter of water weighing 1000kg still contains more hydrogen than a cubic meter of pure liquid hydrogen at 111kg versus 70kg due to the more tightly packed molecules.

Despite hydrogen having a very low volumetric density, the energy density per mass of hydrogen is the highest of all fuels due to its very low weight. When burnt, hydrogen releases 119.93kJ/g (LHV) whereas petrol only contains 44.5kJ/g giving hydrogen an energy density 2.7 times greater than petrol. This still means that the volumetric energy density of hydrogen gas at 1 bar is some 3100 times less than petrol. In other words, the volume of the hydrogen storage required to contain the same level of energy as petrol would have to be 3100 times bigger. This is why hydrogen gas must be stored under compression in order to reduce the size of storage required (see next section on Hydrogen Storage).

Safety is an issue that arises when using hydrogen as a fuel as it is very flammable when ignited with oxygen. Most people think of the Hindenburg disaster when they think of hydrogen safety. However, a NASA employee released a paper citing the zeppelin's skin as the root cause of the accident and the hydrogen fuelled the fire there after.

The flammability of a fuel is often determined between the upper and lower limits of its concentration in oxygen. These limits are referred to by the lower flammability limit (LFL) and the upper flammability limit (UFL). The LFL is the lowest concentration of fuel that will support a self propagating (after ignition source) flame when in the presence of oxygen and the UFL denotes the maximum concentration of fuel in oxygen which can sustain a flame. Above and below these conditions and a flame cannot be supported as the air/fuel mixture is too lean and rich respectively. Stoichiometric conditions are achieved when air and fuel are present in the correct proportions. The diagram below illustrates the range of flammability of hydrogen when compared to other fuels;

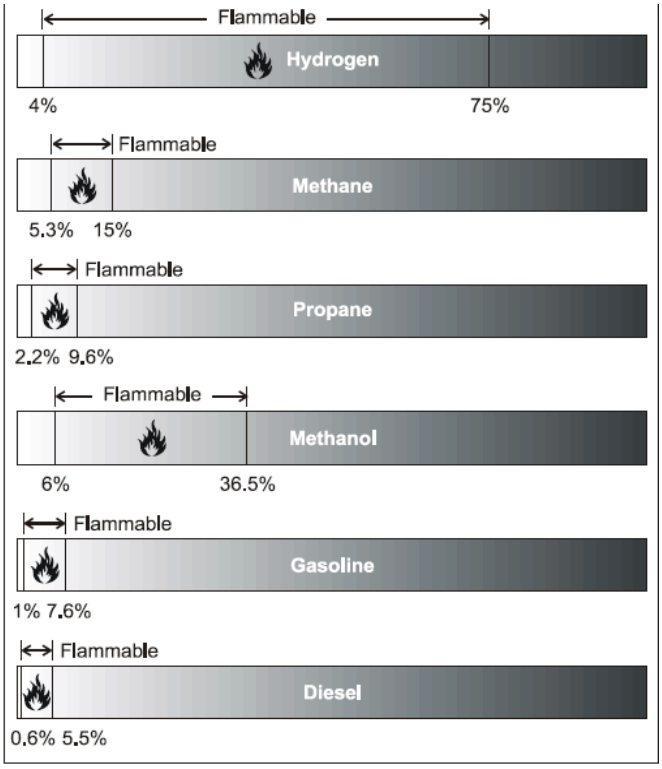

Figure 14 - Range of Flammability [24]

Due to the very small size of the hydrogen molecule, it can leak through very small gaps in containers which otherwise be ait-tight to all other gases. However, should a hydrogen leak occur, due to the very low density under atmospheric conditions and buoyancy it will disperse rapidly up into the air where the concentration of the fuel will quickly fall to a safe level where below the LFL. Should there be a leak in an enclosed area or ignition occur within the range of flammability, the flame will burn upwards and away from the fuel source avoiding setting fire to much of the surrounding materials. This is safer than other liquid fuels where they will pool around the area of the leak and spread the flames outwards rather than upwards.

4.2.5. Hydrogen Storage:

Using hydrogen as an energy source presents a problem when it comes to storage due to the low density issues discussed in the previous section. There are several methods which could be used for storing the hydrogen, each with their own advantages and drawbacks. The most common types of storage in use today are compressed gas storage and cryogenic liquid storage. Other experimental storage types in development are, metal hydride storage, chemical hydrogen storage and carbon-based nano-tubes.

It is proposed in this project that compressed gas storage built from mild steel is used at a pressure of 250 bar (250 times the pressure of standard atmosphere). This would result in the hydrogen only requiring 13 times the volume of storage when compared to petrol for the same energy content rather than 3100 times at 1 bar. 250 bar is a fairly moderate pressure to store a gas when compared to the 800 bar potential of the latest carbon-fibre tanks. However, these latest tanks are being developed primarily for the transport industry so as to keep the size and weight of the vehicle down. In a stationary situation such as this project for supplying fuel cells, the size of the hydrogen tanks are not of as much importance when compared with the transport sector and less energy is consumed in compressing the gas.

Storing hydrogen as a liquid increases the energy density of the hydrogen well beyond that of compressed gas storage. However, the volumetric energy density of these types of storage still can't compete with convention hydrocarbon fuels. In addition to this, liquid hydrogen tanks are more expensive than compressed gas storage, they have issues with loss of hydrogen through 'boil-off' and around 30% of the LHV of hydrogen is consumed in cooling the gas. This makes these systems less attractive for this project but useful in transport situations [25].

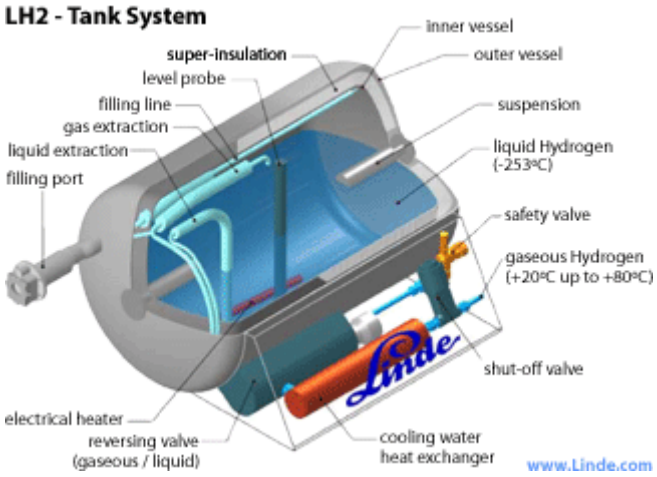

Figure 15 - Liquid Hydrogen Storage Tank [26]

4.3. Heat Pumps:

Heat pumps are a more energy efficient way to provide space heating or domestic hot water heating to a household than conventional methods of using a boiler to heat water or electric heaters. Heat pumps can either use the ambient air (air source heat pumps) as the energy source or geothermal energy (ground source heat pumps). Ground source heat pumps can be split into open loop systems; where the ground loop is circulated at the bottom of a pond or loch, or closed loop systems; where the ground loop is circulated through horizontal trenches a few feet below the frost level or vertically down through bore holes.

It is proposed for this project that closed loop, water to water ground source heat pumps would be more suitable for use on the Isle of Lewis application rather than air source heat pumps. Ground source heat pumps (GSHP) have higher coefficients of performance than air source. The coefficient of performance (COP) is calculated as the energy output from the heat pump divided by the energy input to the compressor and any auxiliary pumps. The COP of a GSHP is between 3 and 4, i.e. the produce 3 to 4 times the electrical energy they consume as heat.

The main advantage of the GSHP is that the geothermal temperature 4-6ft below the frost level remains constant throughout the year. So, in the summer, the ground temperature is generally lower than the air temperature allowing for household cooling if it is needed whereas in the winter, the ground temperature is higher than the ambient temperature. Most households on the West coast of Lewis are spaced out with room in the gardens to install the cheaper horizontal ground loop systems.

Heat pumps operate in the same way in which a refrigerator operates. Low pressure refrigerant is pumped through the closed ground loop heat exchanger (evaporator) where thermal energy is absorbed from the higher temperature soil into the system. The higher temperature refrigerant then returns to the household where it passes through a heat exchanger transferring the heat to the second closed loop system. The fluid in the second loop is then passed through a compressor which raises the temperature (and pressure) to the desired level. The high temperature fluid passes through a third heat exchanger (either another water to water or water to air heat exchanger) which delivers the thermal energy to the home. The thermal energy in the second loop decreases and is then cooled below the temperature of the ground loop through an expansion valve which allows thermal energy to

once again be absorbed from the ground loop heat exchanger. A diagram of this process can be seen in *Figure 16* below;

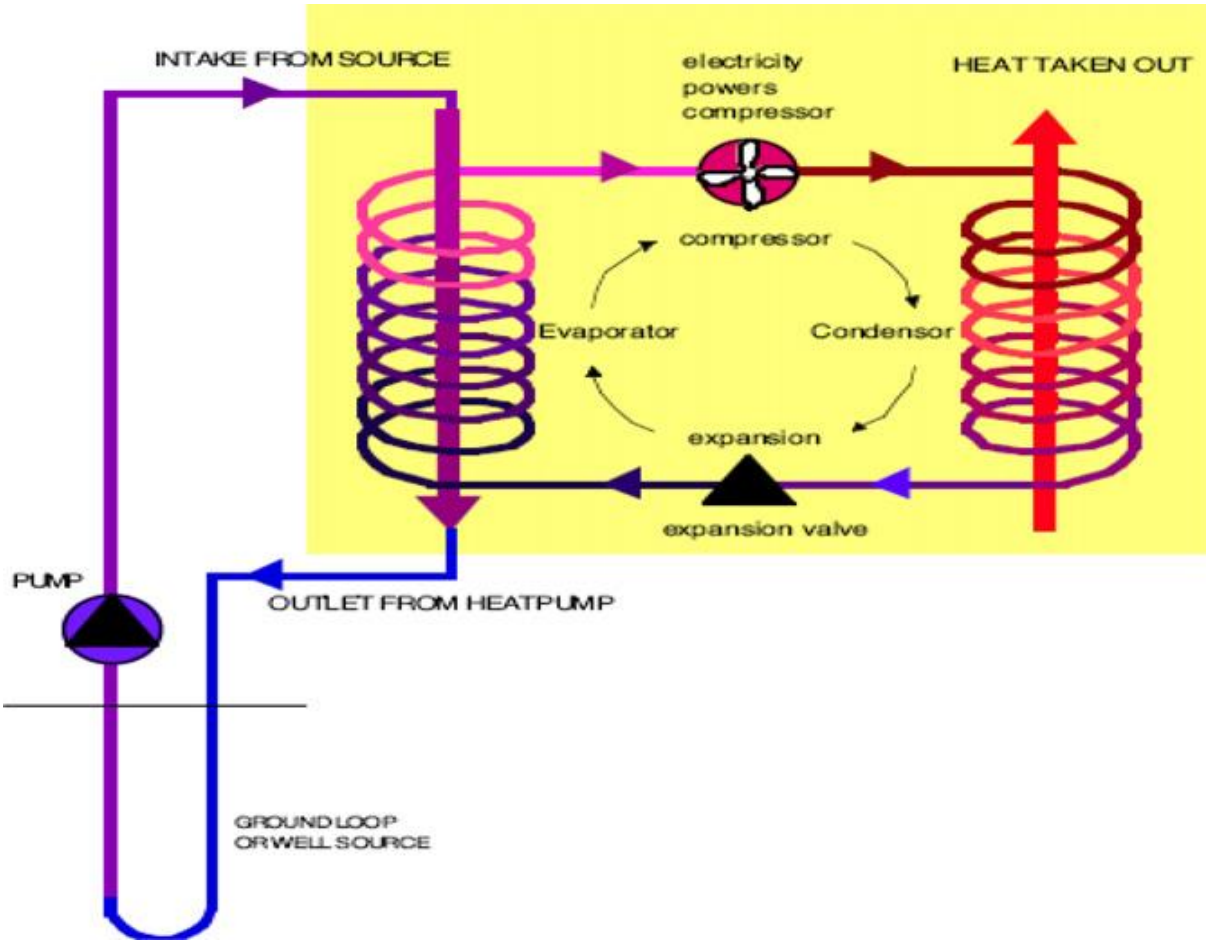

Figure 16 - Ground Source Heat Pump [23]

The theoretical efficiency (or COP) for a heat pump is governed by the second law of thermodynamics and is calculated from the equation 14 below [23];

$$COP_{heating} = \left(\frac{\Delta Q_{Hot}}{\Delta A}\right) \leq \left(\frac{T_{hot}}{T_{hot} - T_{cold}}\right) = 1/\eta_{carnot} \qquad (14)$$

5.1. Project Description:

Introduction to the Isle of Lewis:

The Isle of Lewis is the largest of the Scottish Hebridean islands located off the North West coast of Scotland. At its longest and widest, the island measures 60 miles by 25 miles respectively. The main postal town on the island is Stornoway which has a population of approximately 8000 people with the total Western Isles population estimated at 26,370 in June 2005 by the General Register Office for Scotland (Isle of Lewis accounts for 17,000 of this figure). Lewis is connected to the Isle of Harris to the South which has far more mountainous terrain. The terrain on the Isle of Lewis itself is very flat for the most part. As a result, the island has some of the best sea-level wind energy resource since the wind blows in from the Atlantic Ocean with little obstruction to reduce the incoming energy.

Traditionally, up until the 1970s, domestic energy costs on the Isle of Lewis were fairly cheap due to the abundance of peat available for heating homes and hot water systems. However, since then, a large shift has occurred where homes have been converted to run on fuel oil for heating resulting in a large rise in the cost of energy for the island. The average household on the island uses cheap rate electricity for storage heaters in some of the house and oil fired boiler for the rest. In 2007, it was estimated that around 7 million litres of fuel oil were consumed by the island for domestic heating purposes [27].

There is limited renewable power production on the island at present despite the vast resource and potential for it. A 1MW hydro scheme is installed on the island which provides some of the electricity along with a small wind farm on the Arnish Moor site near Stornoway consisting of 3, 1.3MW Nordex N60 turbines. The sighting of these turbines is a little at odds with legislation that prevents construction of tall structures within a 3 mile radius of the local airport which they are. Many proposals for building large wind farms on the island have been submitted to the local council over the past decade which have met resistance from locals who do not wish the landscape to be spoilt or the habitat for local wildlife. As a result, only the Arnish Moor wind farm exists on the island which is connected to the local grid.

The largest wind farm proposal was made by the Lewis Wind Power Ltd in 2001 which was backed by AMEC and British Energy (now EDF energy). If the project had been accepted, it would have been the biggest wind farm in Europe with a rated power output of 652MW from

181, 3.6MW Siemens wind turbines. Rough calculations released by the project predicted that the wind farm would have produced an annual energy output of 1,997,806 MWh which would have supplied the electrical needs of 425,000 households and saved 1,718,113 tonnes of CO2 per year. These figures suggest that the Lewis Wind Project was taking an average annual household energy consumption of 4700kWh which is fairly consistent with the UK national average. However, due to wind's intermittent nature and the fact that energy produced during low demand times (night-time) is likely to be dumped as the grid cannot store electricity, the actual output figures would look less favourable but it does provide an indication of the wind farm's performance. Along with the Lewis Wind Power proposal, two other large wind farms were proposed from Scottish & Southern Energy and Beinn Mhor Power which would have taken the total installed wind capacity on the island to 1016MW [28].

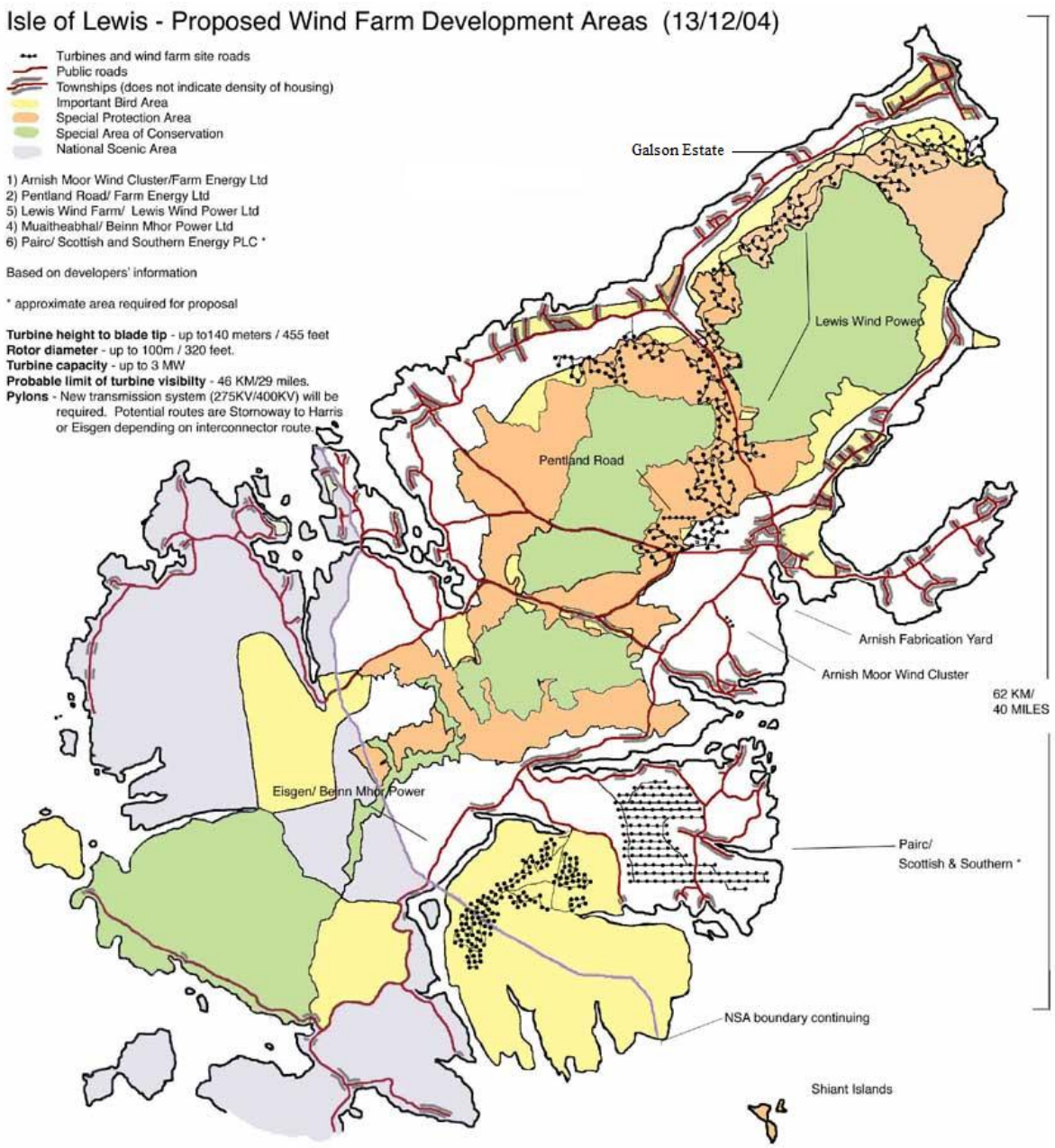

Figure 17 - Proposed Wind farms on Lewis [30]

The map above the shows the location of the proposed wind farms mentioned previously. This map was produced in 2004 and only the Arnish Moor wind cluster to the South of Stornoway was constructed. The location of the Galson Estate project has also been indicated on the map. The Pentland Road wind farm is a project that has been in the making for five years but has problem with the Airport and environmentalist concerned about the habitat of the Golden Eagles. Allowing the construction of any one of these wind farms would have resulted in many jobs being created on the island. Furthermore, the Arnish steel fabrication yard was used in the construction of the Arnish Moor wind farm and would once again be

used for the new wind farms which would give the local company very useful business to keep them afloat as one of the mainstays of the Western Isles economy [31].

Isle of Lewis Grid Connection:

The Isle of Lewis is connected to the National Grid via a 33kV transmission line entering North Harris from a sub-sea cable running from Ardmore on the Isle of Skye. The total capacity of the current transmission cables is approximately 30MW with the minimum demand load never dropping below 9MW [29]. The 33kV transmission line runs up the middle of the island with an 11kV network supplying the small villages dotted along the roads and closer to the coasts. The 2.73MW wind farm installation proposed in this project would free-up some of the limited power capacity on the local grid leading to fewer power cuts for the residences on the end of the lines.

5.2. Galson Estate Wind Data:

As was mentioned in the introductory section, the Galson Estate is located on the West coast of the island along the main road that heads to the most Northern tip in Port Ness. A meteorological site has been set up on the estate by the Galson Trust in combination with the engineering department at Lews Castle College which is part of the University of Highlands and Islands.

Lews Castle College supplied this project with wind data collected in 10 minute intervals from the Galson Estate meteorological site which is located 10 meters above ground level. This data revealed that an average wind speed over the entire year from March 2008 to March 2009 was measured at 7.03m/s which is within the expected value for the location. The Weibull distribution chart of the wind speed is shown in the figure below.

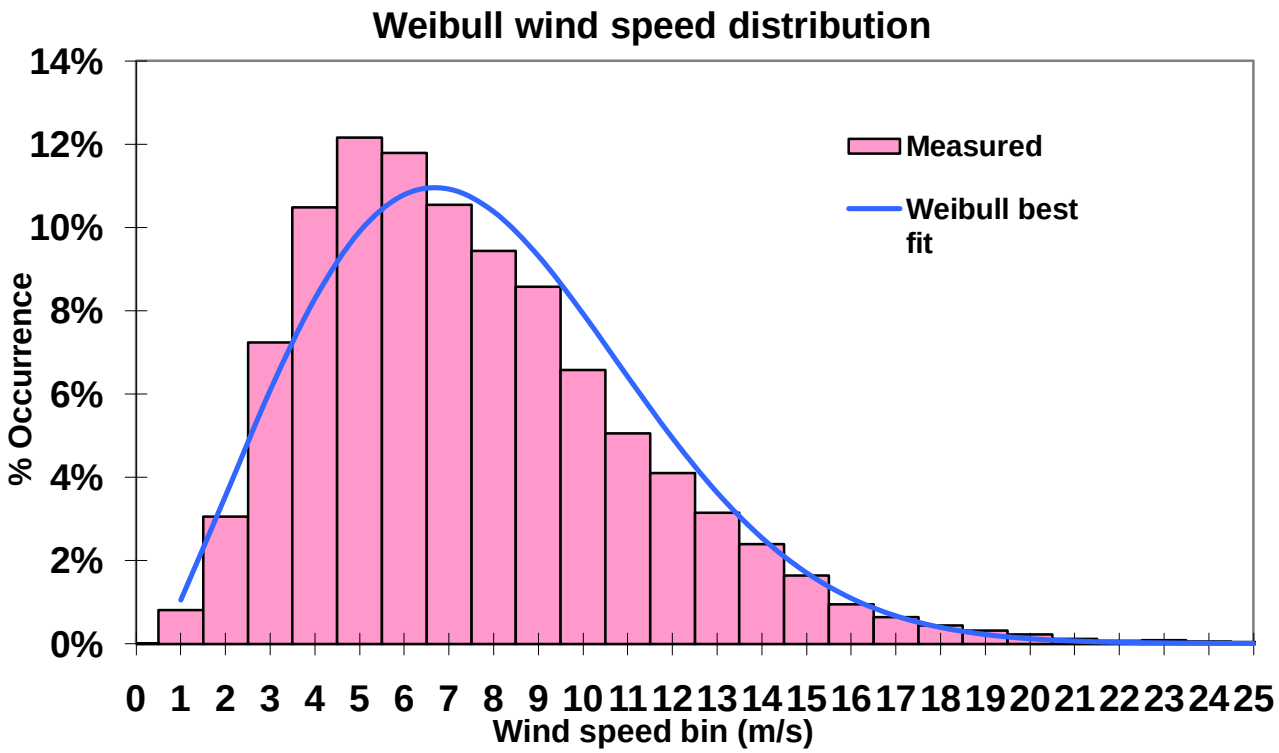

Figure 18 - Galson Estate Weibull Distribution

The Weibull distribution illustrates the frequency of a wind speed over the year which can be used to select an appropriate wind turbine that produces the greatest energy at the most frequent wind speeds [22]. The equation for creating the Weibull distribution graph in the figure above is shown here in equation 15;

$$w(v) = \frac{k}{c}\left(\frac{v}{c}\right)^{k-1} \exp[-\left(\frac{v}{c}\right)^{k}] \qquad (15)$$

Where v is the wind speed, k (calculated as 2.16 for the Galson estate) is the shape factor and c (calculated as 8.23) is the scale parameter.

Since the standard height for meteorological weather station is used on the Galson Estate (10m above ground level), the wind speeds need to be scaled up to for the hub height of the Enercon E44 wind turbines being used in the project. These turbines have a hub height of 55 meters. The wind speed needs to be scaled up due to the wind shear factor (boundary layer) present close to ground level. Wind speeds are affected by wind shear up to heights of approximately 100 meters above ground level. The speed of the wind flow increases from stationary (on the ground) up to the full free stream flow above 100 meters. The logarithmic formula used to calculate the wind speed at the 55 meter hub height is shown here in equation 16;

$$V_2 = V_1\left(\frac{LN\left(\frac{Z_2}{Z_0}\right)}{LN\left(\frac{Z_1}{Z_0}\right)}\right) \qquad (16)$$

Where V_2 is the new wind speed at the 55 meter hub height, V_1 is the original 10 meter wind speed, Z_2 is the new hub height, Z_1 is the original height and Z_0 is the roughness factor. The roughness factor refers to the type of landscape obstructions present around the wind farm. For the Galson Estate, it was assumed that a roughness factor of 0.03 would apply to the

fallow fields of the area. The new average wind speed for the site over the year was calculated at, 9.09m/s (up from the original 7.03m/s).

Using the wind power curves available from Enercon for the three 0.91MW turbines, the hourly energy output from the wind farm can be calculated from the new scaled up wind data. It was found that the capacity factor (or load factor) for these turbines on this site is 37.3% which is better than the UK average (25-30%). The capacity factor relates to the actual annual energy output from the wind turbines divided by the theoretical maximum energy output if the turbines were to operate at their rated power all year round. The total monthly energy output from the three turbines can be seen in *Figure 19* below;

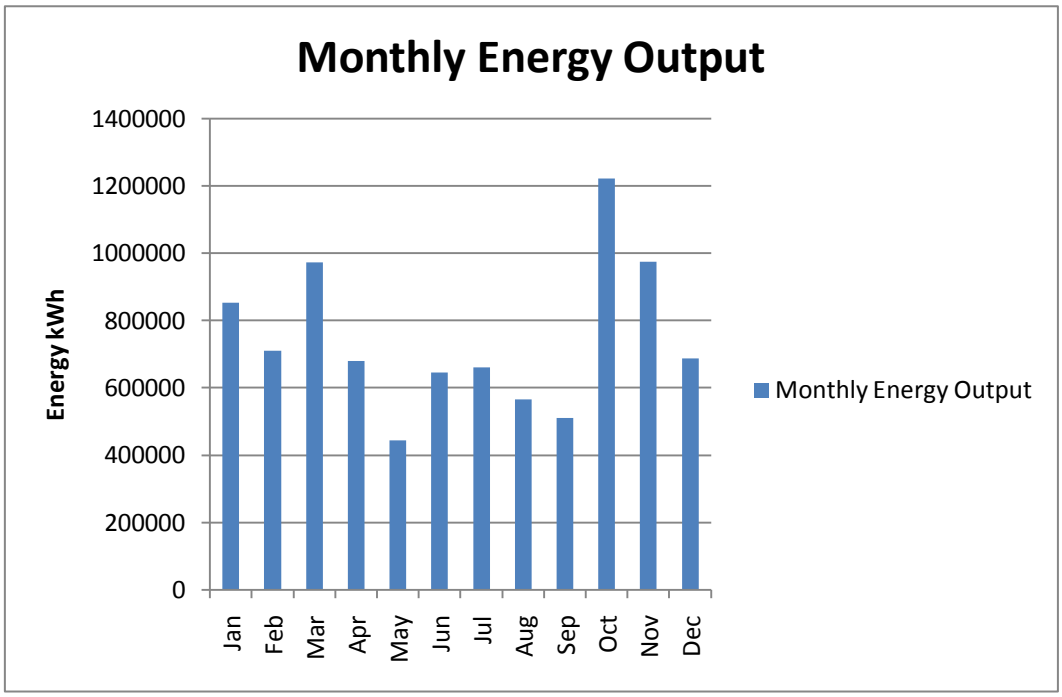

Figure 19 - Monthly Energy Output from Wind Farm

This graph illustrates the difference in energy output from the wind farm over the year. It can be calculated that the average energy produced by the wind farm in the summer is 583406kWh compared to 838206kWh in the winter. The average energy produced in the winter is 44% greater than it is in the summer. This is a useful correlation to note since the energy demand in the winter is comparatively higher than in the summer due to the increased

requirement for lighting as a result of the fewer daylight hours and electric space heating if installed in the house.

5.3. Heat and Power Demand:

5.3.1. Electrical Power Profile:

Contact was made with an employee (Donald Mackenzie) of Scottish & Southern Energy on the Isle of Lewis with regards to obtaining annual hourly electrical demand data from the Barvas substation which supplied the whole North-West corner of Lewis with electricity. A request was made to Scottish & Southern headquarters in Perth to release the data to the public domain to be used in this project. However, time constraints for the submission of this thesis meant that the data could not be used as it failed to arrive before the project deadline.

Instead, an electrical profile generating tool developed by an MSc project group from Strathclyde University was used as a substitute [32]. The tool uses simple user defined inputs for a particular community such as, number of households and total energy consumption. Percentages of ownership of typical electrical appliances, occupancy level of households in community and occupancy frequency are input into the generator where probabilities calculate the times and duration of use of each appliance to generate hourly electrical demand profiles for the four seasons.

It was estimated in 2005 that the average total energy consumption per household in the UK over a year is 21,500kWh (heat and power). Of this figure, 12,250kWh (gas central heating/cooking) are used for space heating, 4600kWh for domestic hot water and 4650kWh for electricity demand [27]. It should be noted that the actual electrical energy consumption per household used for electrical appliances and not heating will be lower (~3500kWh) than this figure since some houses use electric heating. This gives a mean energy demand per hour of 2.45kWh although peak power demands will be significantly higher than this figure.

Donald Mackenzie from Scottish & Southern Energy indicated that the average annual electricity consumption per household for the North-West corner of Lewis will be in the region of 7500kWh (3500kWh for electrical appliances and 4000 kWh for electric heating). This 7500kWh figure was used in the calculations for the electricity demand profile. The diagram below, *Figure 20* - Daily Power Profile (1 house), represents the daily electrical demand profile for 1 household on the Galson Estate on the Isle of Lewis over the four seasons. From the graph, it appears at first glance that the Spring profile is missing; however, the profile is present on the graph but is hidden for most of the day behind the Autumn profile since these

seasons were calculated to be fairly similar. The thickness of the line representing the Autumn profile was decreased slightly in order to reveal more of the spring profile.

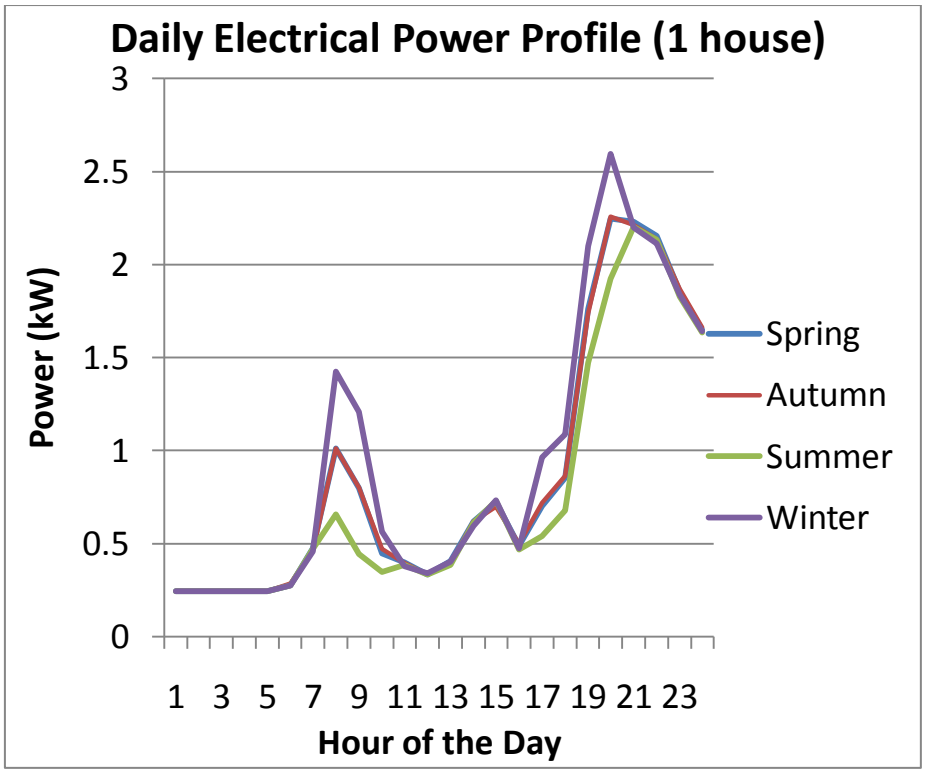

Figure 20 - Daily Power Profile (1 house)

5.3.2. Heating & DHW Profiles:

It was hoped that actual hourly heating demands for the year would be attained for the project to match the hourly time-step of the wind-hydrogen system in the Excel program however, the best that was achieved was monthly heating energy totals from a typical house on the island.

The figures provided were from a local couple (Brian and Kath Griffiths) who obtain their heating energy requirements for most of the year from a 2.5kW micro-wind turbine installed in their back garden supplying the DC current to electric heaters in the house. The data supplied for this project dates from 2003, before the installation of the wind turbine.

Incidentally, since 2003, the couple has managed to reduce their annual heating energy consumption down from 14,805kWh to 9,500kWh through energy savings methods and changing their energy usage behaviour. The figure below illustrates the monthly energy consumption for a typical household on the island;

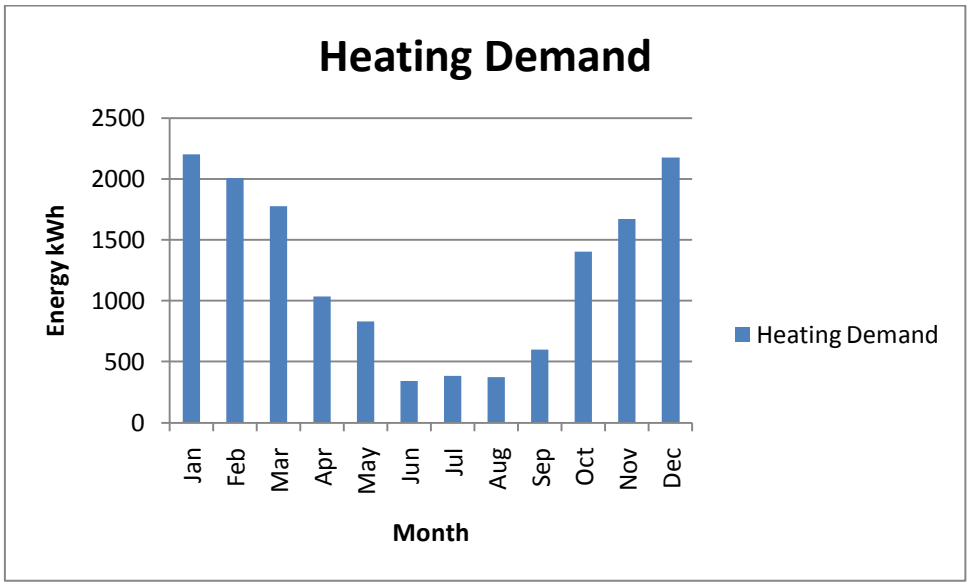

Figure 21 - Monthly Heating Energy Demand

Domestic hot water consumption was assumed to be constant throughout the year so the same daily hot water consumption was applied throughout the simulation. In 1979, scientists (Perlman and Mills) carried out a study focussed on modelling domestic hot water use profiles. It was found that the average household consumes 245 litres of hot water every day for use in washing dishes, cooking and hygiene (showers and baths) [33].

The temperature in a domestic hot water tank in the UK is required to be 60^{o}C even though showers and baths require a temperature of approximately 40^{o}C. The reason for this is to prevent the growth of the Legionella bacteria which causes Legionnaire's disease in humans (can be a fatal form of pneumonia) [34]. The Legionella bacterium needs warm water conditions in which to grow between the temperatures of 20^{o}C and 45^{o}C.

Below is the profile for domestic hot water consumption in a typical household;

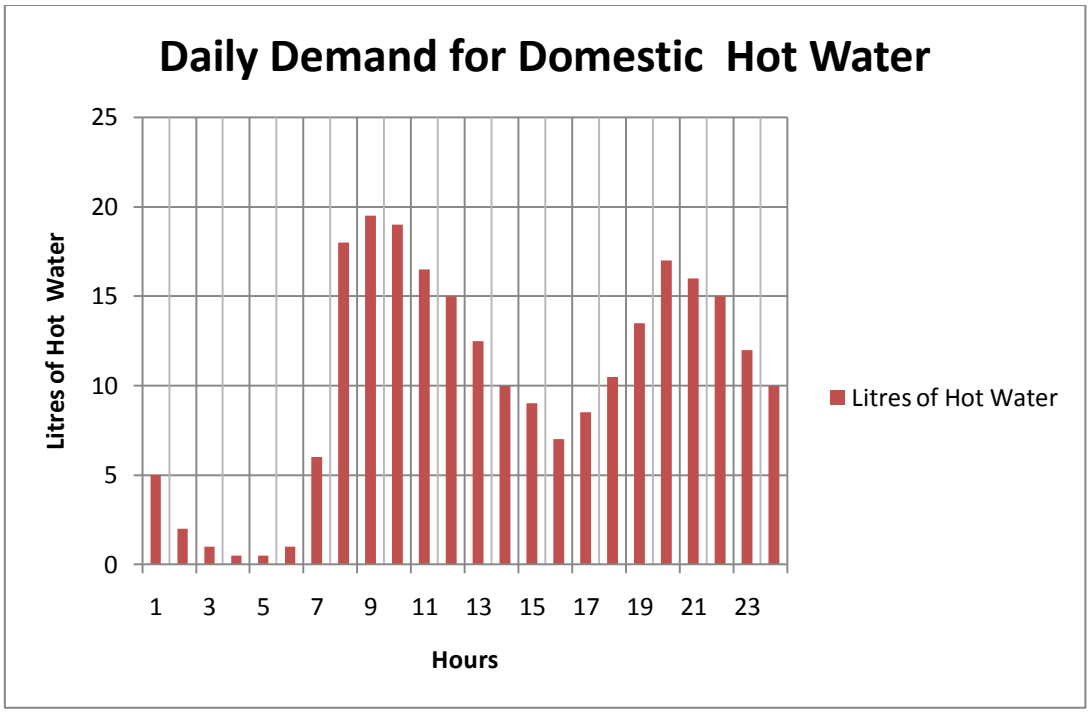

Figure 22 - Daily Demand for DHW

5.4. UHI/Greenspace Research Hydrogen Systems:

5.4.1. Introduction:

The data for the performance of the PEMFCs to be used in this wind-hydrogen project (and also the PEM electrolyser) was obtained from experimental results. These experiments were carried out in the Lews Castle College hydrogen laboratory where access to hydrogen fuel cell was gives as well as a hydrogen gas producing electrolyser to ensure efficient was always available in the gas storage.

As discussed in section 4 of this paper, manufacturers will and proponents of fuel cell technology often quote high efficiency ratings. These high efficiencies are normally achieved at optimum loading ratios on the fuel cell and likewise, on the electrolyser. It is far more useful to know how these systems perform during a wide range of transient loading ratios. As such, this will result in more accurate results for the wind-hydrogen simulation since the fuel cell and electrolyser will need to operate under transient load conditions; the fuel cell needs to follow the varying electrical demand from the household and the electrolyser needs to absorb the excess energy produced by the wind farm.

5.4.2. Hydrogen Systems:

The Lews Castle College (LCC) hydrogen laboratory is fitted with range of safety devices to avoid any incidents involving a hydrogen gas leak in the room. The fire door was kept closed at all times and the room was fitted with a raft of hydrogen gas detectors. The hydrogen storage cylinder was located outdoors in a locked cage so that the fuel source was kept out of the building. When a hydrogen leak is detected in the room, the electronic safety shut off valve closes stemming the flow of any more hydrogen entering into the room as well as cutting the mains electricity supply to the laboratory. Then, a series of high powered suction fan vents (located on the roof where the hydrogen would collect in the event of a leak) are turned on to rapidly remove the gas from the room and eliminate the chance of ignition. Should a fire start in the room, there is an automatic fire extinguishing system present to prevent the spread of the fire. The image below is of the safety control unit for laboratory including the electronic hydrogen shut off valve, the switch for the gas extraction system and the mains power supply cut-off switch produced by siGEN;

Figure 23 - LCC Hydrogen Laboratory Safety System

The hydrogen in the storage cylinders was generated using a 6kW electrolyser from an Italian company (Idrogen[2]) which used a DC electrical current supplied from the grid. However, the Greenspace Research facility has a renewable energy croft containing micro-wind turbines and solar photovoltaic panels on the same land plot as the College which could theoretically supply the energy to the electrolyser. This would clearly generate hydrogen from renewable energy sources rather than the usual method of obtaining hydrogen from steam methane reforming. The electrolyser was away receiving maintenance in Italy during the project, however, there was still sufficient hydrogen stored in the 1Nm^3 steel cylinder (at 15 bar of pressure) for the experiments to be carried out and a back-up 1kW electrolyser was being installed in the meantime. The energy contained in the storage tank was approximately equivalent to 45kWh. The image below, *Figure 24*, is of the large electrolyser containment

unit outside the building which is located next to the hydrogen fuel storage cylinder shown in the subsequent image, *Figure 25*.

Figure 24 - Electrolyser Containment Unit

Figure 25 - Hydrogen Storage Tank

The hydrogen in the tank shown above was used to supply the high purity fuel (99.999% purity) to the fuel cells in the hydrogen laboratory. The fuel cell being used in this investigation was a product from the German manufacturer, Heliocentris. The fuel cell can produce a design peak power output of 600W through a DC output of 13.3V at a current of 45A. The fuel cell has its own pressure regulator which can accept up to 15 bar of hydrogen. During experimentation, the hydrogen gas pressure supply to the fuel cell was kept at ~8 bar to ensure reliable operation using external pressure regulators (from fuel gas specialists, Air Products) incorporated into the main hydrogen supply system in the laboratory. The following image illustrates two of the three external pressure regulators in the laboratory set to deliver 8 bar of pressure. The hydrogen purge pipe shown in the image leads to another valve which when opened, releases any gas pressure caught in the system into the atmosphere after the two manual fuel valves and electronic valve are closed.

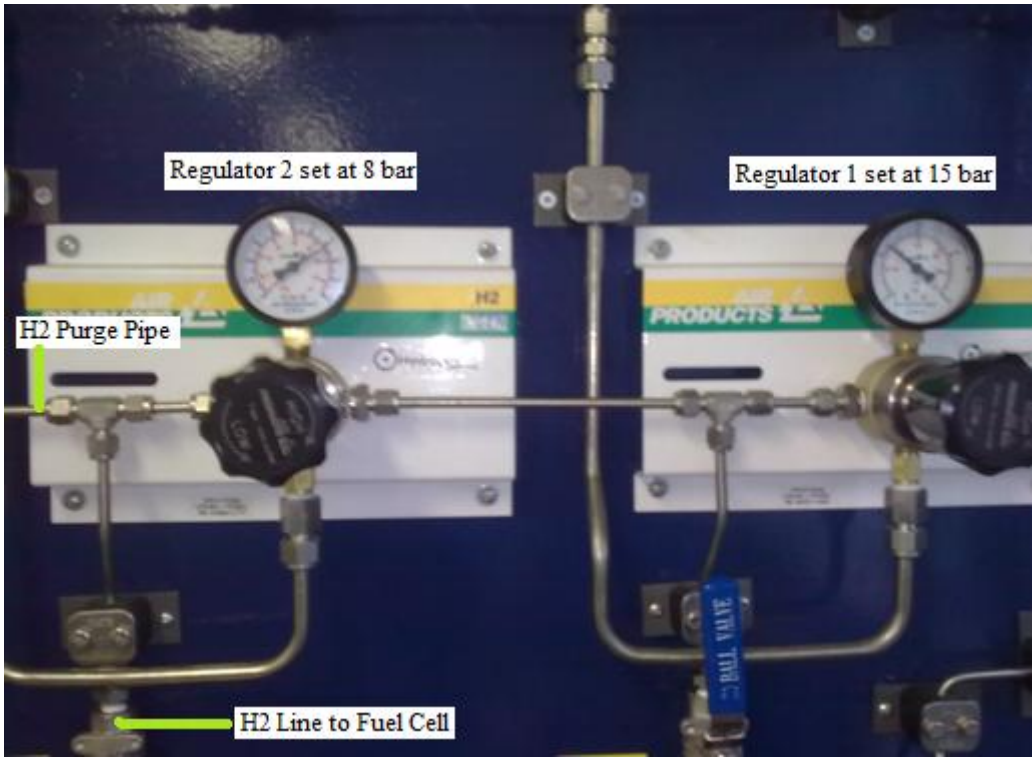

Figure 26 - Hydrogen Laboratory Pressure Regulators

The fuel cell stack comprised of 24 individual cells which were kept from overheating via a closed water cooling loop. The maximum permissible stack temperature is 70^{o}C, above which, and the fuel cell goes into a safety shutdown procedure. Similarly, if any of the individual cells falls below 70% of the maximum voltage output from the other cells, then the system will again enter a safety shutdown procedure.

The coolant loop for the fuel cell has a water reservoir which feeds into an electric pump, supplying cooling water to circulate around the fuel cell stack. The pump supplies a steady flow rate of approximately 1600ml/min of water coolant to the fuel cell. The coolant then leaves the stack where it passes through an air to water heat exchanger. The heat exchanger has two cooling fans mounted on one the top side and a large, finned surface area which radiates some of the thermal energy stored in the coolant into the atmosphere. Temperature measuring equipment is fitted to the coolant pipes at the entry and exit of the fuel cell so that the heat exchanger efficiency can be determined.

The cathode electrodes of a fuel cell require a supply of air (containing the necessary oxygen) to complete the energy producing chemical reactions which occur inside the stack. On

smaller fuel cells up to around 50W capacity, the air in the atmosphere is enough to complete the reactions, however, larger fuel cells such as the one being used in this project require an air fan to circulate air through the bipolar plates to the cathode electrodes.

The fuel cell unit is completely energy self sufficient requiring no external power supply. The electrical power required for the ancillary systems in the unit (water pump, cathode air supply fan, heat exchanger fans and integrated electronic control/measurement panel) comes from the fuel cell itself. The fuel cell charges a 12V battery which supplies the energy to the ancillary systems.

Fuel cell power output responds to electrical loading being placed on the external circuit. The fuel cell used in the laboratory is capable of producing unregulated DC power, regulated DC power (achieved with the use of an integrated DC-DC converter holding a minimum 12V output by varying the current) and 230V AC power (with the use of an integrated DC/AC inverter).

The system control panel was set-up to log data from various sensors in the system and output the information to a desktop PC where all the data could be monitored in real-time (1 second time intervals) using LabVeiw software. The data available from the system included; FC stack voltage current and power, battery voltage and current, stack temperature, coolant inlet and outlet temperature to the stack, available fuel gas pressure, volume flow rate of coolant, cathode air circulation and fuel cell management current (parasitic loading on the stack from the ancillaries). The data from LabView could be recorded and output to an Excel file for post analysis.

A hydrogen gas flow meter was fitted between the fuel cell pressure regulator and the mains hydrogen fuel supply. Unfortunately, the LabView software designed for monitoring the gas flow meter data on a PC was an outdated version and operated at a different bit rate to the communications port in the more modern PC. Ultimately, the gas flow meter was not essential as the fuel consumption of the stack can be calculated after the experiments from the fuel cell electrical efficiency.

The image below is of the fuel cell used in the experimentations for this project;

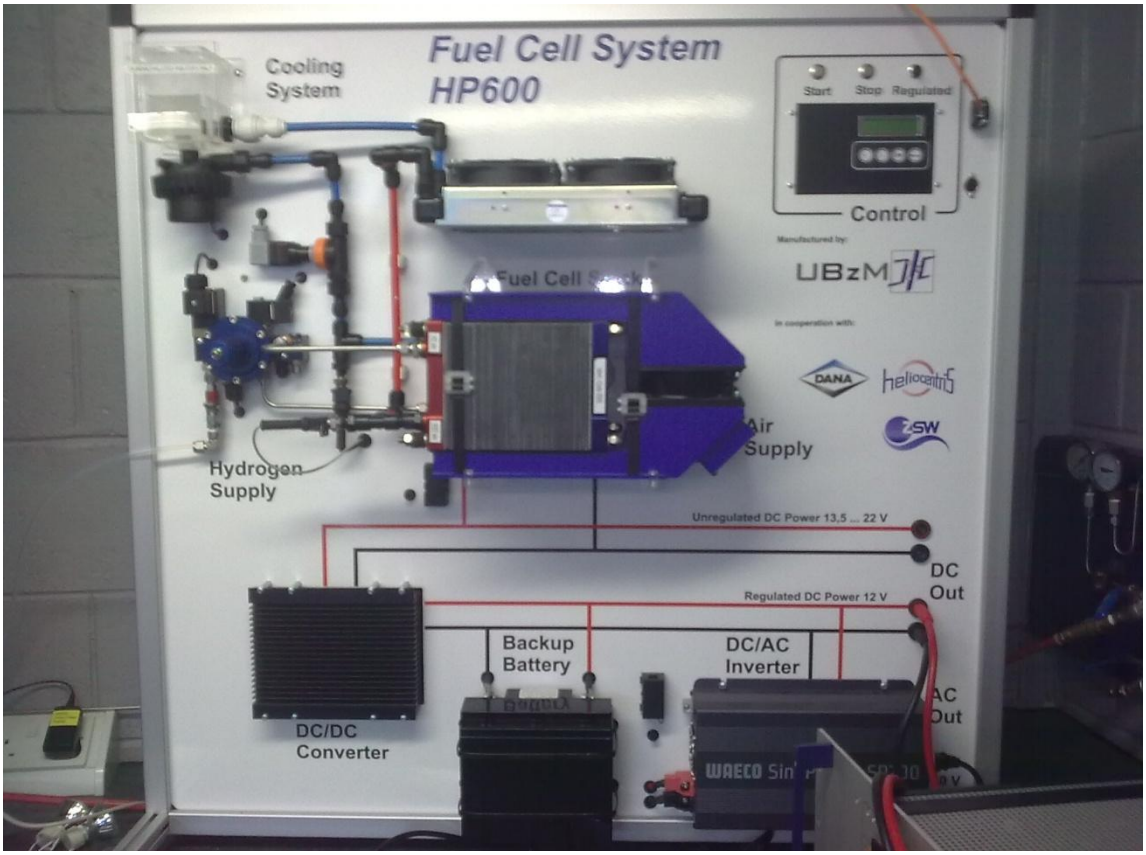

Figure 27 - HP600 Fuel Cell System

As can be seen in the figure above, positive and negative electrical cables are connected to the regulated DC output from the fuel cell. These cables are connected to an electronic load capable of applying a peak power load of 1500W to the fuel cell which is more than the fuel cell can produce. The experiments on the fuel cell were carried out by gradually increasing the current on the electronic load panel over the fuel cell's operating range. The following image in *Figure 28* is of the electronic load unit also built by the same company as the fuel cell, Heliocentris;

Figure 28 - Electronic Load on Fuel Cell

6. Experimental Results:

6.1. Introduction:

The simulations for the project were carried out using Microsoft Excel and the Visual Basic Editor for some of the processes. The simulations were carried out in hourly time-steps over the year using the Galson estate wind data from 2008 as detailed in section 5.

The primary aim of the simulations was to discover the maximum number of households the proposed 2.73MW wind farm could supply with all of the electrical energy presently required by the houses in the community stretching up the North coast from South Galson to Port Ness. The maximum number of households was determined using an iterative process until there was no unmet electrical load in the system. The electrical demand profiles being used in the simulation also contain a total of 3500kWh over the year per household in electricity used for space heating.

It is intended that the energy produced by the wind farm will first be used to serve the electrical demand from the community through a local grid. Any surplus energy generated delivered to mini hydrogen stations which are distributed out over the community area involved in the wind-hydrogen scheme. The fuel depot in Stornoway which currently stores the oil used by households on the island contains several tanks in the region of $100m^3$ in volume. This is common for remote island towns as they must rely on oil rather than a gas network for their heating energy. It is thought that each compressed hydrogen storage container would be of this size.

Using a distributed hydrogen station approach would minimise the energy losses in the transmission of the fuel as the electricity in the grid is the only energy that would need to travel any great distances as opposed to piping the hydrogen to the community or transporting it with vehicles. It would, however, necessitate the construction of a local hydrogen piping network to connect the fuel cells in the homes to the fuel supply.

Each hydrogen station would consist of a rectifier (change the incoming AC power to DC for the electrolyser), a PEM electrolyser, a small hydrogen tank to act as a buffer between the electrolyser and the compressor, a diaphragm-type compressor which subsequently feeds the main hydrogen storage tank.

Referring to *Figure 20* in section 5, it can be seen that each household in the community will require a fuel cell with a rated capacity of 3kW to be able to guarantee the supply of power to the home throughout the year when the energy from the wind farm is insufficient. These fuel cells will also require power conditioning in the form of an inverter to convert the DC power produced by the stack into the AC power used in the home. In addition, the fuel cell cooling circuit will pass through a contra-flowing water-water heat exchanger where the thermal energy in the stack coolant is transferred to the incoming mains water destined for the dwelling's hot water tank. This will have the effect of pre-heating the domestic hot water using the waste heat in the coolant so that less energy is required to bring the tank temperature up to the required 60^{o}C.

The map below illustrates the area of the community that electrical demand profiles have been generated for. Scottish & Southern Energy estimates that there are 1000 households in this area connected to the grid;

Figure 29 - Community Area for Wind-Hydrogen Project [35]

6.2. Technical Results and Analysis:

6.2.1. Wind Farm:

The energy output from the system is clearly governed by the wind resource and the efficiency of the installed wind capacity at capturing the wind resource. Below shows the wind power curve used in the simulation to obtain the hourly energy outputs from the wind farm of 3 turbines over the year;

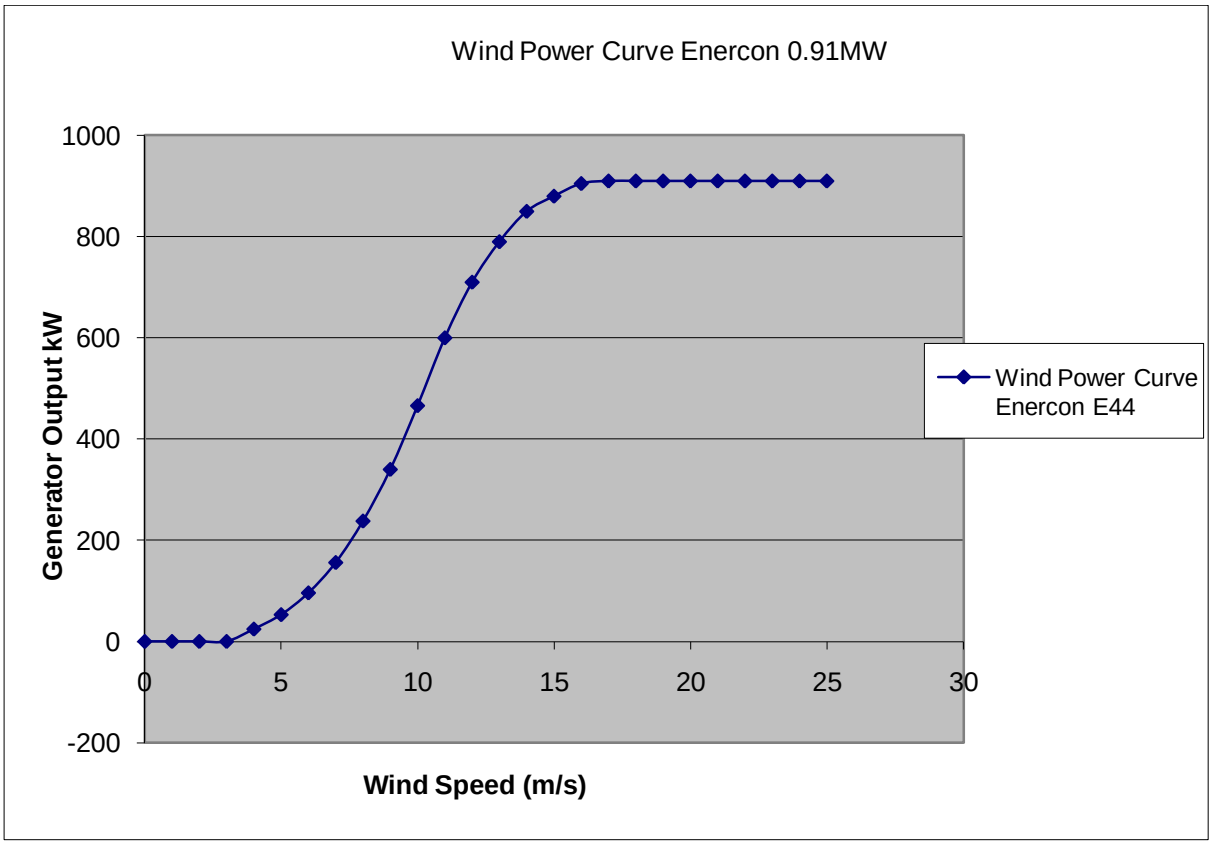

Figure 30 - Enercon E44 Power Curve

The cut-in and cut-out wind speeds of the turbine are 4m/s and 25m/s respectively. There are three periods in the summer when the wind farm produces very little energy which puts a strain on the system as the community will need to rely on the stored energy in the hydrogen tanks. The first period occurs at the beginning of June where the system must solely depend on the fuel stores for 36 hours. The next occurrences of no and very little energy from the

wind farm occur in July for durations of 29 hours and 37 hours. Surprisingly, the longest period without energy from the wind farm is 103 hours in December. However in reality, when the electrical demand of the community is applied to the simulation, there will be far longer periods where energy from the hydrogen tank will be relied upon to meet the load.

Table 2 Shows some of the details from the wind farm where the CO_2 savings are calculated based on a figure of 0.86 tonnes per MWh and the average UK household consumes 4700kWh;

Theoretical Wind-Farm Output	Actual Wind-Farm Output	Capacity Factor	Average Wind Speed (Hub Height)	Total Cumulated Days Without Power	Theoretical No Average UK Households	Annual theoretical CO_2 Savings
23,915 MWh	8,925 MWh	37.32%	9.1m/s	43	1900	7676 tonnes

Table 2 -Wind Farm Results

6.2.2. Experimental Results from Fuel Cell:

The results obtained from experimentation on the 600W fuel cell were scaled up by a factor of 5 to represent the 3kW fuel required in each household in the full system energy balance. The electronic load unit discussed in section 5 was first connected to the power conditioned DC output (DC-DC converter), and then in a later experiment to the unregulated DC output where the load on the fuel was ramped up in 2.5A increments between 0A and 70A and the performance was recorded.

The aim of the experiments was to determine the electrical efficiency of a PEM fuel over transient load conditions as well as recording the coolant output temperatures from the stack. The results from the regulated DC output experiments provided the most reliable data from the fuel cell which could be continuously repeated to achieve the same results each time. The table below shows truncated results of the parameters recorded in the experiments deemed most important to this project;

Load Current (A)	FC Voltage (V)	FC Current (A)	FC Efficiency (%)	Thermal Output (W)	Coolant Inlet Temp (^{o}C)	Coolant Outlet Temp (^{o}C)
0	19.4	2.1	65.7	21.3	28	28
10	16.0	12	54.2	162.2	31	32
20	14.7	22.2	49.8	329	37	39
25	14.3	25.6	48.4	389.6	42	45
30	13.8	31.5	46.7	495.2	46	49
35	13.4	33.7	45.4	543.2	50	56
40	13.2	35.9	44.7	585.9	51	56
45	13	37.9	44	626.1	51	56
50	12.9	38.6	43.7	641.5	51	56
60	12.1	42.4	41	738.6	51	57
70	11.4	47.1	38.6	853.5	52	58

Table 3 - Experimental Fuel Cell Results

As can be seen from the table, the peak efficiency of a PEM fuel cell is at minimum loadings which is not at all useful for delivering power to a load. Installing over-sized capacity fuel cells relative to the peak demands would be one option to operate the unit higher up its efficiency curve, however, as can be seen in *Figure 32*, the unit would need to be greatly oversized to achieve reasonable increases in efficiency at great capital cost to the project since the efficiency rapidly deceases at low loadings before levelling out.

The efficiency of the fuel cell was calculated from equation 11 in section 4 where the fuel utilisation factor was assumed to be 0.98 and the LHV of hydrogen was taken as 1.23V(in terms of ideal electrolyser [19]) was multiplied by the number of cells in the stack. The efficiency figures refer to the electrical efficiency of the stack. It is assumed that there are no hydrogen leaks in the system, therefore, the energy lost is in the form of heat. The thermal output is simply calculated by taking into account both the fuel cell stack power (obtained from P=IV) and lost energy suggested by the electrical efficiency.

It is noticed that the condition where zero external load is placed on the fuel (0A entry in table 3), still results in the fuel cell doing some useable work. This can be attributed to the parasitic power consumption mentioned in section 5 where the fuel cell management systems (FCMS) draws energy from the battery to drive the ancillary systems.

It was discovered when increasing the load on the fuel cell using the electronic load unit that there came a point where the load power being drawn from the fuel cell was exceeding the fuel cells maximum rated power output (600W). The fuel cell entered a safety shutdown procedure when a peak load of 70A and 10.1V (707W) was exerted on the stack. This was some 107W higher than the rated power of the fuel cell. It was realised that when the load exceeds the output of the fuel cell, the FCMS draws on the 12V back-up battery to meet the additional load. The fuel cell only shutdown since the battery reached a critical state of charge where it entered an energy preservation routine. This affected the results from the experiments as it is expected that the power output from the stack increases gradually to a maximum before tailing off beyond this maximum loading point. The voltage power curves from the fuel cell experiment can be seen in *Figure 31* below;

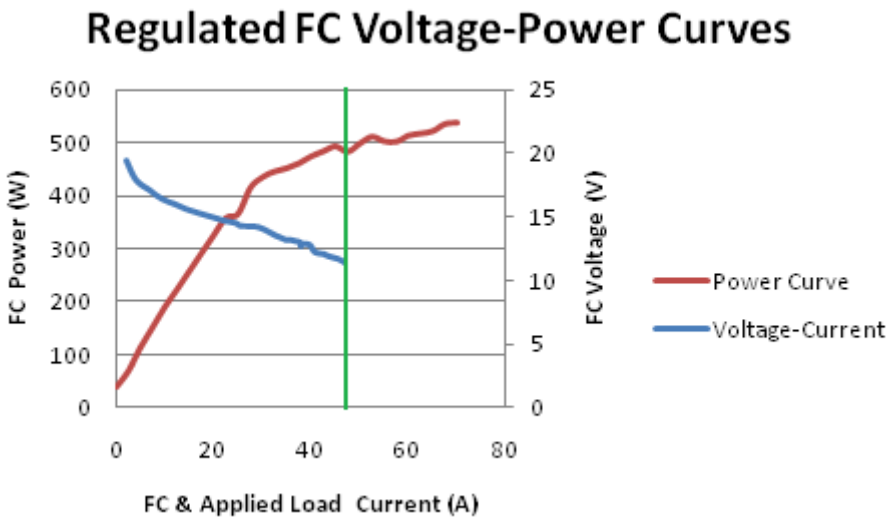

Figure 31 - Fuel Cell Voltage Power Curves

The instruction manual for the fuel cell was consulted to determine where the voltage power curves transitioned from being the product of solely the fuel cell stack to being a combination of the stack and battery. The green line in the figure above illustrates this point and shows where the fuel cell power begins to dip. The voltage and power curves up to this point are characteristic of a PEM system. This information was then used and the applied load was converted in to a percentage to produce the corrected efficiency curve seen below in *Figure 32*.

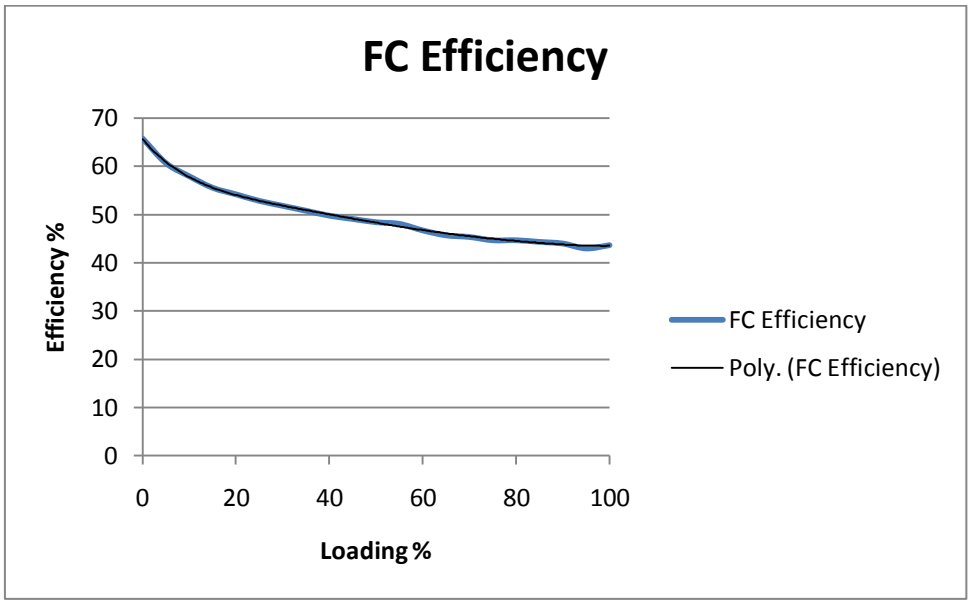

Figure 32 - Corrected FC Efficiency Curve

The efficiency curve in the figure above contains a 6^{th} order polynomial curve which was used to gain a mathematical expression for the curve in Excel. It was found that the 6^{th} order polynomial equation accurately follows the fuel cell efficiency curve between the loadings of 0 and 22% (where the biggest slope change in the curve occurs). Beyond a loading of 22% and a simpler 2^{nd} order polynomial equation more accurately represents the straighter part of the curve. These equations were used in the overall system energy balance where the efficiency of the fuel cell unit could be determined at any demand loading value. The two polynomial equations can be seen here below as equations 16 and 17;

$$y = 3E\text{-}10x^6 - 1E\text{-}07x^5 + 1E\text{-}05x^4 - 0.0011x^3 + 0.0449x^2 - 1.1408x + 65.622 \quad (16)$$

$$y = 0.0023x^2 - 0.4106x + 62.712 \quad (17)$$

The practical experiments that were planned for the project were to evaluate the operating efficiency of a PEM fuel cell which was achieved as discussed above. It was also hoped that experimentation of electrolyser efficiency could be carried out in the hydrogen laboratory but since the unit was unavailable during the project, (away for maintenance) this was not possible in the end. However, as it is a PEM electrolyser that is to be used in the project, the efficiency results from the fuel cell experiments were applied to the reverse process of the electrolyser as well.

6.2.3. Gas Compressor Model:

A simple thermodynamic mathematical model for a diaphragm compressor was adopted from another hydrogen energy project carried out by the European Commission and Institute for Energy [36].

The model was used to determine the power requirement from the system to compress the hydrogen produced by the electrolyser at 1 bar to 250 bar for storage. The inlet conditions to the compressor were assumed to be 1 bar of pressure and 15^{o}C ambient gas temperature (288K). Equation 18 below is used to calculate the theoretical amount of work required for the gas compression;

$$W_{theory} = \left(\frac{\gamma}{(\gamma-1)}\right) * Z * R_{H_2} * T_0 * [(P_1/P_0)^{\frac{(\gamma-1)}{\gamma}} - 1] \qquad (18)$$

Where γ is the adiabatic exponent for a diatomic gas (1.41), Z is the compressibility factor at the inlet to the compressor (1.001), R_{H_2} is the hydrogen gas constant (4.124kJ/molK), T_0 is the inlet temperature in Kelvin (288), P_1 is the required outlet barometric gas pressure and P_0 is the barometric inlet gas pressure. Now, from the solution to equation 18, the theoretical work can be used to calculate the actual unit work required for the compression of the gas. This is obtained from equation 19 as follows;

$$W_{Actual} = a * \left(\frac{W_{theory}}{\eta_c}\right) * \rho_{H_2} \qquad (19)$$

Where η_c is the typical efficiency of diaphragm compressor (figure of 80% was used in this simulation), 'a' is a conversion factor changing kJ to kWh (1/3600) and finally, ρ_{H_2} is the density of hydrogen gas assumed to 0.0899kg/m^3. The solution to equation 19 gives the unit work required for the gas compression in this project as 0.508kWh/Nm^3.

6.2.4. Electrical Power System Energy Balance:

The simulations carried out for the total energy balance of the electrical power system were based on the wind-hydrogen system being able to deliver power all year round to the community. The system also needed to maintain a minimum hydrogen storage tank state of charge of 10%. This would provide the system flexibility in the case that wind resource in subsequent years varied slightly from the 2008 data. Having the 10% minimum state of charge would also allow the system to absorb any fluctuations in peak demand. In reality, since the electrical demand curves for the community were generated based on theory, (see section 5.3.1 for details), the system will not have any of sudden peaks in demand will occur during the year.

As has already been discussed, the system will take any wind energy generated from the farm and deliver it directly to the local grid feeding the households. This ensures maximum efficiency of the system as it would be highly inefficient (both financially, due to the large hydrogen system required, and energy inefficient) to supply all the energy through the buffering system. Some of the energy produced by the wind turbine is lost through the power conditioning units required to feed the AC power from the generator to the grid at the correct frequency. From the wind turbine section in section 4, the Enercon E44 wind turbine has its synchronous generator decoupled from the grid, first with the use of a diode base rectifier to change the voltage to DC and then with the use of pulse width modulation using insulate gate bipolar transistors (IGBTs). These systems have typical conversion efficiencies of 95% which have been adopted in this project [37]. There are further losses due to power conversion at the hydrogen stations converting the AC grid power to DC for the electrolyser and with the household fuel cell needing DC-DC converter followed by a DC-AC inverter. These efficiencies were also assumed to be 95% [38].

When there is a surplus of electricity from the wind farm, it is converted to hourly available DC power in Excel. This available surplus must be split into energy required to drive the diaphragm gas compressor and energy for the electrolysis of water. The energy used for the electrolysis of the water was converted into a percentage of the rated power input to the fuel cell so that the polynomial equations, 16 and 17, could be used to determine the volume of hourly volume of hydrogen produced over the year. The total rated electrolyser size was calculated from the hourly maximum available energy from the wind farm surplus minus the

energy required for the compressor and rounded up to the nearest 100kW. The compressor power required was calculated at 8.63% of the available energy surplus which corresponded to the average electrolyser electrical efficiency over the year of 51.3%.

When there is a deficit between the power produced by the wind farm and the electrical demand from the community, the 3kW fuel cells located in each household balance the load by consuming hydrogen from the storage tanks. The peak electrical power demand from a household over the year is found to be 2.6kW from the demand profile shown in *Figure 20*. Therefore, there is capacity in the 3kW fuel cell to cope with some variances in the actual peak demand experienced over the year. The total hourly required power conditioned output from the fuel cells are calculated in Excel from the deficit between wind farm output and electrical demand. From this, the required input energy to the fuel cell (in the form of hydrogen fuel) can be calculated using the same method as for the electrolyser. Equations 16 and 17 are used to accurately plot the efficiency curve of the PEM fuel cell based on the percentage loading calculated from the rated power output from the fuel cell. The total rated power output from the fuel cell systems is obtained by simply multiplying the number of households in the community by the rated power of one fuel cell.

The system is assumed to have hydrogen fuel in its storage tanks at the beginning of the year so that the fuel cells can be used if required before the system has a chance to produce any hydrogen fuel itself. In fact, for the first four hours of the year, the wind farm produces no energy so the fuel cells are relied upon to deliver the energy to the load using the hydrogen placed in the tank at the start. From running a few iterations of the simulation, a starting energy content of 180,000kWh is chosen to be placed in the tank. This is equivalent to 5350kg of hydrogen by mass or 240m^3 by volume under a pressure of 250 bar. The energy balance that occurs in the hydrogen tank takes the form of equation 20 below where the hydrogen tank efficiency is assumed to be 99% efficient;

$$Hydrogen\ Tank\ Energy\ Balance = (Ely_{out} + H_{2_{Stored}} - FC_{Req}) * 0.99 \qquad (20)$$

Where Ely_{out} is energy content in the hydrogen produced by the electrolyser, $H_{2_{Stored}}$ is the energy stored in the hydrogen tank from the previous hour and FC_{Req} is the energy consumed by the fuel cell for that hour.

A macro was set-up using the Visual Basic editor in Microsoft Excel to change the size of the community (and therefore the energy demand) to a user defined input. Using this method, the maximum number of households that the wind-hydrogen system could supply could be determined whilst maintaining a 10% minimum hydrogen tank storage level. Additionally, the program was set-up to obtain the various component sizes required for the particular size of system being investigated as well as their performances.

It was found that the 2.73MW wind farm could meet its primary aim of delivering all of the electrical power demands to a community of 432 households with a total energy demand of 3,257 GWh over the year whilst maintaining a minimum tank state of charge of 10%. If the tank were allowed to almost completely empty, the system could cope with an additional 8 houses at 440 with a total electrical energy demand of 3,318 GWh. The following table demonstrates some of the outputs from the wind-hydrogen system for the 432 households and 440 household scenario.

Outputs	**432 Households**	**440 Households**
Total Demand (kWh)	3,257,301	3,317,621
Total Wind Energy Available (kWh)	8,925,096	8,925,096
Wind Energy Delivered to Load (kWh)	2,153,376	2,184,374
Wind Energy Delivered to H_2 System (kWh)	6,009,192	5,979,744
Energy Consumed by FC (kWh)	2,319,903	2,382,134
Energy Delivered by FC Electrical (kWh)	1,133,718	1,164,003
FC Thermal Output (kWh)	1,186,185	1,218,131
Energy Consumed by Compressor (kWh)	518,620	516,079
Energy Consumed by Electrolyser (kWh)	5,490,572	5,463,655
Number of FC Operating hours	3065	3097
Number of fuel cell starts	452	458
Overall Fuel Cell Efficiency (%)	48.87	48.86
Overall Electrolyser Efficiency (%)	51.31	51.28

Minimum Tank Level (%)	10.18	0.295
Maximum H_2 Tank Size Required (m^3)	756.4	667.4
Required FC Size (kW)	1296	1320
Required Electrolyser size (kW)	2200	2200
Required Compressor Size (kW)	210	210
Unmet Electrical Load (kWh)	0	0
Energy in tank at Year End/Surplus (kWh)	409,727 / (229,727)	335157 / (155,157)
CO_2 Emissions Savings (tonnes)	2801	2853
Overall Electrical Efficiency of System (%)	36.5	37.2

Table 4 - Electrical System Results

The overall electrical efficiency shown at the bottom of table 4 takes into account the energy left in the hydrogen storage tank at the end of the year. Since the storage tanks start with a combined total of 180,000 kWh of energy in them at the start of the year, there must be at least 180,000 kWh of gas left in the tank at year end. With both scenarios, there is more energy left in the yank at year end that at the start of the year. The surplus energy figures are shown in brackets in the table. This hydrogen could be siphoned off from the tank and sold as a fuel to another market (e.g. transportation project on the island).

Inevitably, there is a small difference in the required fuel cell rating between the two scenarios, but the 440 household system required a smaller storage tank than the 432 household system. This can be explained by the smaller community system being required to never drop below a minimum storage tank state of charge of 10%.

With the system never dipping below 10.18% state of charge, there is an energy reserve in the system of 58,157 kWh. The average energy demand over the year for the 432 household scenario is 372 kWh. Taking this into account, there is enough energy in reserve to run the whole community for 156 hours or just under a week. When the hydrogen tank is at its maximum capacity of 756.4Nm^3, there is enough energy to support the community for 63.5 days at the average hourly demand of 372kWh.

The maximum hydrogen tank size required for the 432 household scenario can be assumed to be 800m^3. With the proposed tank sizes for the system of 100m^3, there will need to be 8 hydrogen generating stations spread out over the community which will each serve a

community of 54 houses each. The size of the other individual components in each hydrogen station would be; 275kW electrolyser/inverter and a 27.5kW compressor. The average daily state of charge of the hydrogen tank throughout the year can be seen in the figure below;

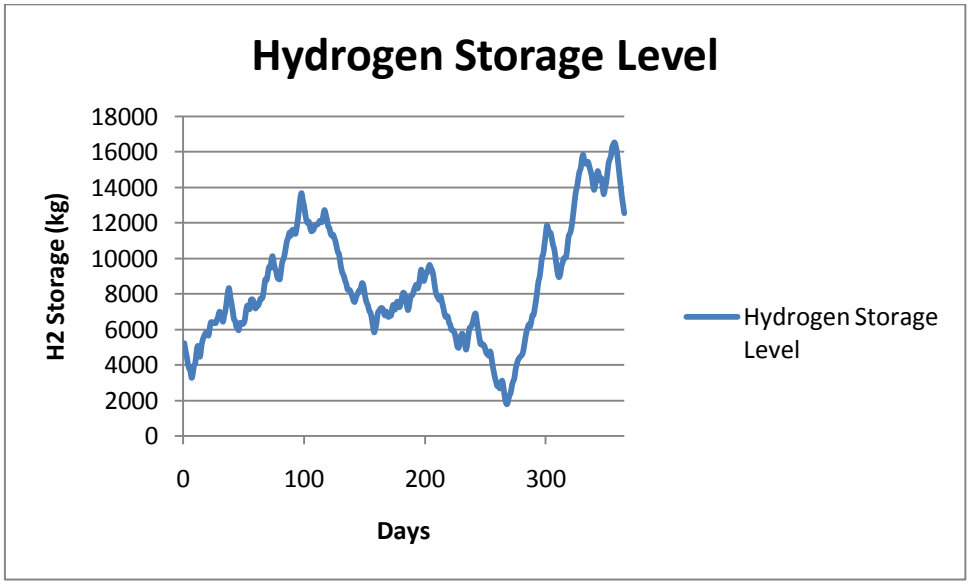

Figure 33 - Hydrogen Storage Level

The general trend from the graph illustrates that the hydrogen storage is replenished during the spring and winter months while the lower wind speeds from the middle of the year result in a net decline in the fuel storage. This is also reflected in an increase in fuel cell activity during the middle part of the year. Referring back to *Figure 19*, the energy output from the wind farm is at its lowest throughout the year during the month of May. The fuel cell is predictably most active during this period. As mentioned above, the average hourly energy demand from the community is approximately 370 kWh. During the month of May, the average demand is slightly higher at 378kWh. The fuel cells are relied upon to deliver almost half of the energy during this period at an average energy output of 186kWh.

Stationary fuel cells can have operational lives lasting up to 40000 hours. The fuel cells in this project are required for 35% of the year (just over 3000 hours/year) which would suggest that they have a lifespan of approximately 13 years. However, the conditions that the fuel cells are operating under are more reflective of PEM fuel cells used in transport applications.

The fuel cell is required to operate at continuously variable loadings in this project as they would be in a transport application and they make over 400 start/stop procedures over the year. These types of operating conditions tend to lead to shortened life expectancies meaning that a 13 year life-span is over optimistic.

6.2.5. Thermal Energy Recovery for DHW and Heating:

The secondary aim for the system was to determine how much of a household's annual space-heating and domestic hot water energy requirements could be supplied by the wind-hydrogen system. This would be achieved through the use of heat recovery from the fuel cell's coolant circuit in a heat exchanger to pre-heat the water destined for the domestic hot water tank. Additional energy would then need to be imported from the electrical grid to power an emersion heater in the hot water tank to achieve the required 60^{o}C temperature in the hot water tank.

The electricity demand curves for the community contain a large portion of energy that is normally consumed in electric heaters. Instead of using this energy to directly supply electric heaters, it could instead be consumed by a ground source heat pump (discussed in section 4) to increase the heating potential in the household. There is 3500kWh of available energy in the power demand curves used in the simulations. Assuming coefficients of performance from the ground source heat pump between 3 and 4, the fuel cell could potentially supply heating energy to the household over the year between 10500kWh and 14000kWh. According to the monthly heating demand averages shown in *Figure 21*, the fuel cell could supply roughly supply between 71% and 95% of a household's annual heating requirements.

Heat Recovery Result from Fuel Cell:

The results from the experiments on the 600W fuel cell can be seen in *Table 3*, along with the output temperatures of the coolant from the stack. The outputs from the 600W fuel cell can be scaled up by a factor of 5 to mimic the performance of the 3kW fuel cells intended for use in the households. Peak output temperatures for systems of this size tend to be between 80 and 100^{o}C. For this reason, a temperature scaling factor was also applied to the experimental results so that under peak loading, the coolant outlet temperature reaches 80^{o}C.

In section 5, the annual domestic hot water heating energy consumed by a household in the UK is 4650kWh. It is assumed for this project that the average mains water inlet temperature on Lewis is 10^{o}C and the volume consumed per day is 245 litres (*Figure 22*). So, knowing the mass of water, the inlet temperature and the desired outlet temperature (10^{o}C and 60^{o}C

respectively), the annual energy required for domestic hot water heating can be calculated from equation 21 below;

$$Q = C_p * m_{water} * dT \qquad (21)$$

Where Q, is the heat required, C_p is the specific heat capacity of water, m_{water} is the mass of water and dT is the difference in temperature. Using a C_p value of 4186J/kgK, a mass of water of (245*365=89,425kg) and a temperature difference of 50 degrees Kelvin, gives an annual energy requirement of 5199kWh per household or 14.24kWh per day. However, the outlet temperature from the fuel cell is much higher than the mains water temperature therefore; the domestic hot water can gain useful energy from the wasted heat in the fuel cell coolant.

Since the heat exchanger fitted to the 600W fuel cell during the experimentations was of the wrong type for this application (water-air), the actual heat transfer for the water-water heat exchanger will need to be estimated from calculations. The average effectiveness was taken to be 0.75 for the system which would be applied to the maximum heat transfer equation to obtain the household heat exchanger outlet temperature.

The coolant water mass flow from the fuel cell was scaled up by a factor of 5 from the experimental results (1600ml/min) to represent the 3kW fuel cell (0.133kg/s). The mass flow rate from the mains water supply into the heat exchanger was calculated as (0.068kg/s). This corresponds to the daily mass of hot water consumed by a household passing through the heat exchanger during one of the fuel cells' operational hours. The outlet temperature of the domestic hot water from the heat exchanger is calculated from the equations below;

$$C_{min} = m_{dotcold} * C_{p_{cold}} \qquad (22)$$

Where $m_{dotcold}$ is the mass flow rate of the mains water heading to the hot water tank and $C_{p_{cold}}$ is the specific heat capacity of the water at 10°C. The maximum heat transfer can now be calculated using equation 23 below;

$$Q_{max} = \varepsilon * C_{min} * (T_{hot_{in}} - T_{cold_{in}}) \qquad (23)$$

Where ε is the heat exchanger effectiveness and the two temperatures relate to the hot coolant entering the heat exchanger and the cold mains water. From this equation, the outlet temperature of the water heading to the hot water tank can be determined using equation 24;

$$T_{cold_{out}} = T_{cold_{in}} + \frac{Q_{max}}{C_{min}} \qquad (24)$$

Applying these equations across the outlet temperatures obtained from the experiments carried out on the fuel cell gives the outlet temperatures from the heat exchanger. These results are presented in the *Figure 34* below;

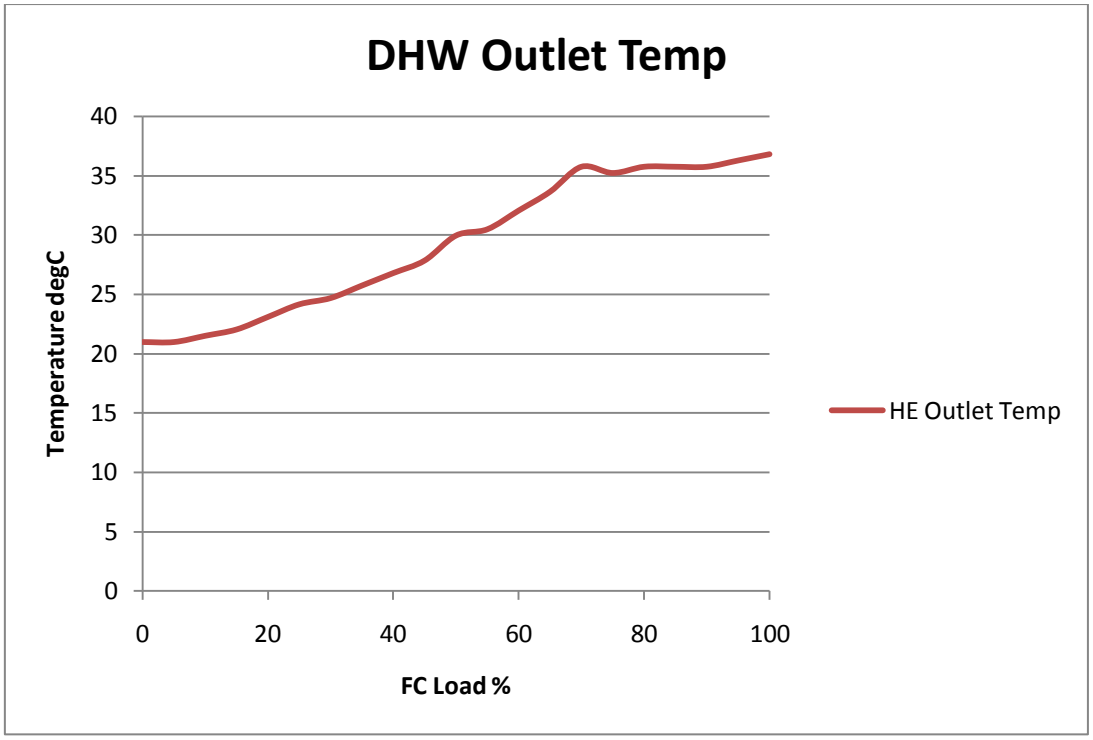

Figure 34 - DHW Outlet Temperature

The same method was used for obtaining the heat recovery from the fuel cell as for applying the fuel cell and electrolyser efficiency curves to the simulation. Two polynomial equations were used to model the heat recovery curve as shown in the figure above. A third order polynomial equation was used to accurately model the curve in the figure above up to a fuel cell loading of 67%. Above a loading of 67% and a simpler second order polynomial equation is used to model the flatter part of the curve. These two equations are shown below;

$$y = -4E\text{-}05x^3 + 0.0057x^2 - 0.0098x + 21.016 \quad (25)$$

$$y = -0.0004x^2 + 0.2314x + 19.255 \quad (26)$$

The table below shows the results from the heat recovery calculations;

Outputs	432 Households
Total Energy Required for DHW heating (kWh)	2,319,839
Total Energy Recovered (kWh)	773,004
Total Additional Energy required (kWh)	1,546,835
Total Fuel Cell Efficiency (%)	82.2
Total System Energy Efficiency (%)	45.2

Table 5 - Heat Recovery Results

The table above demonstrates the increase in total efficiency of the fuel cell when operating as a CHP device rather than purely for power generation (up from 48% to 82%). The total system energy efficiency improves by 9% of pure power generation making the entire power system over 10% more efficient than a single cycle fossil fuel power station. With the use of heat recovery, 33% of the annual energy required for DHW heating is supplied from the wasted heat in the coolant of the fuel cell.

A 12 to 18% reduction in domestic hot water energy consumption could potentially be made on top of the heat recovery system being fitting further heat exchangers to the bath and shower drainage pipes. These pipes contain hot water, known as grey-water, whose thermal energy could be recovered to further optimise the community wind-hydrogen system [39].

Figure 35 shows the average daily energy recovery (by month) from the fuel cells as well as the additional energy required to heat the water in the tanks up to 60^{o}C;

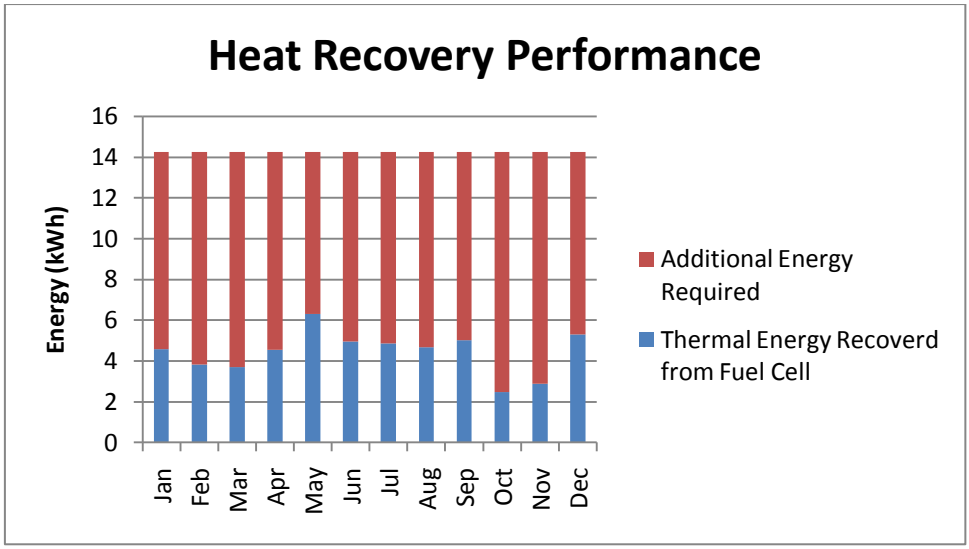

Figure 35 - Heat Recovery Performance

Clearly, the thermal energy recovered from the fuel cell is representative of the fuel cell activity throughout the year. Therefore, in times of low wind resource, the additional heating energy required for the DHW will be less due to the operation of the fuel cell. From the figure above, it is known that the wind resource is poorest during the month of may and at its best October and November which is reflected in the heat recovery performances shown.

6.3. Economic Analysis of Component Costs:

A brief analysis of the capital costs related to the component sizes of the system detailed in section 6.2.4 is presented here. This analysis purely looks at the capital costs associated with the components in a wind-hydrogen system rather than the large costs that would be involved in setting-up such a system with the installation of a grid connection to the wind turbines and a local hydrogen gas piping network (since residences do not rely on natural gas at present).

The table below details the costs that would be involved in the optimal 432 household scenario. The life-span of the wind farm is considered to be 20 years so some components will need replacing during the project. The figures for the costs involved were taken from a recent project on a similar topic which used various manufacturers' quotes [40].

Component	Capital Cost (£)	Replacement Cost (£)	Operational & Maintenance Costs (£) / Year	Total (£)
Wind-Farm	3,052,932	N/A	45,794	3,968,812
Fuel Cells	3,110,400	2,954,880	62,208	7,309,440
Electrolysers	5,280,000	4,752,000	105,600	12,144,000
Compressors	198,800	N/A	2,982	258,440
H_2 Storage	23,800,000	N/A	595,000	35,700,000
Power Conditioning	3,496,000	N/A	52,440	4,544,800
Total	**£38,938,132**	**£7,706,880**	**£864,024**	**£63,925,492**

Table 6 - System Component Costs

It can be noted from the table above that the cost of the wind farm nearly 13 times less than the costs required for the hydrogen systems despite the wind farm being the energy source for the community. However, it is clear that the costs of the 8 large, compressed storage tanks needed to store the fuel required to support the community during times of low wind resource are the primary costs associated with the system. As technology improves and wind-hydrogen

systems become more common, the capital and maintenance costs of this type of scheme should begin to fall.

7. Conclusions & Recommendations:

Conclusions:

The Isle of Lewis has a significant amount of un-tapped wind energy resource which could be used to help meet the UK's renewables targets in 2020. This project looked to address the issues of intermittent power supply from wind farms with the use of a wind-hydrogen system.

The proposed wind farm by the Galson Trust on the West coast of Lewis is theoretically capable of supplying 1900 UK average households with electricity. However, the intermittent nature that wind farms generate power with means that the actual number of households which the wind farm can supply energy to all year round is zero.

It was found that with the use of a hydrogen system, the wind farm could supply the electrical energy needs of 432 households all year round whilst never allowing the hydrogen fuel storage to drop below 10% full. This represented an electrical system efficiency of 36.5% with an energy surplus at the yearend of 229,727kWh (enough energy to support the entire community for 26 days without any wind power). The environmental impact of this is a CO_2 saving of 2801 tonnes per year.

Eight hydrogen generating stations are needed in the system which are distributed over the community demand centres thus minimising energy losses in transmission. Each station would contain a 100Nm^3 storage capacity capable of supplying the electrical energy needs to 54 households.

Results from heat recovery calculations carried out on the fuel cells indicate that a significant improvement in overall fuel cell and entire system efficiency can be made. The fuel cell efficiency improves to 82.2% and overall efficiency is up to 45.2%. These are useful improvements in efficiency considering the relatively modest fuel cell output temperatures that contribute to 33% of the a household's annual DHW energy requirements.

Finally, a brief look into the capital costs of the wind hydrogen system components revealed that the size of the hydrogen storage tanks were the main influencing factor on the £38,938,132 figure.

Future Recommendations:

- The simulation of the wind energy system related electrolyser efficiencies to the experimental fuel cell efficiencies as the electrolyser was unavailable during the project. For future work, it would me more accurate to experiment with the efficiency of the electrolyser with the transient power supplies to obtain more representative results. This could be achieved between Greenspace Research and Lews Castle College by supplying the energy for electrolysis from the power generated on the renewable energy croft they have on-site.

- The heat recovery potential from the fuel cell could also be explored with experimentation. The households on the island require 3kWel fuel cells with heat recovery potential. A useful progression to the project would be to work with a 3kW PEM fuel cell and have the coolant circuit passing through a water-water heat exchanger being supplied with mains water as the heat sink for the coolant.

- Obtaining hourly demand data for households in the community for space heating would be another logical progression in moving towards a 100% renewable community. Greenspace Research has an open system ground source heat pump under development in their renewable energy croft. Carrying out experiments over the year with this system would provide more accurate efficiencies of the heat pump in the Lewis climate which could be applied to wind-hydrogen community to optimise the energy available from the wind farm.

- The Isle of Lewis has often been linked with the construction of large wind farms in excess of 100MW (larger than the 2.73MW farm investigated in this project). For this reason, it may be useful to look into a wind-hydrogen system of a much larger scale to learn how this could be integrated into a renewable energy of this size.

- The wind-hydrogen system modelled in this project was found to produce excess hydrogen by the end of the year. Future work in this area could look into the possibility of beginning a renewable transportation project using hydrogen as the fuel. At present, the Western Isles council are keen to get such a project into action. They

are in discussions with the Royal Mail van service on the island based in Stornoway to introduce one or two vans using hydrogen in the internal combustion engines rather than petrol. In addition to this, the market for oxygen gas could be looked into since the electrolysis process produces large quantities of oxygen gas. On Lewis, one possible industry which could make good use of stored oxygen gas is the fish farming industry where managing the O_2 concentration in the water enhances fish production.

References:

[1] ReStats: Renewable Energy Statistics Database for the UK, (Website 2008-2009). Available from: http://www.restat.org.uk/electricty.html

[2] House of Commons Innovation, Universities, Science and Skills Communication. Renewable Electricity-Generation Technologies (5th Report of Session 2008-2009). Date: 11th June 2008

[3] Carbon Trust Strategy: The UK Renewable Energy Strategy 2009, (Website 2009). Available: http://www.carbontrust.co.uk/../CarbonTrustBriefingonUKRenewableEnergyStrategy2009.pdf

[4] The Ashden Awards for Sustainable Energy: Wind Energy Summary, (Website 2008). Available from: http://www.ashdenawards.org/wind

[5] A Norwegian Case Study on the production of Hydrogen from Wind Power, International Journal of Hydrogen Energy (30th November 2006). Authors; Christopher Greiner, Magnus Korpas and Arne Holen.

[6] Utsira Wind Power & Hydrogen Plant, (1st July 2004). Norsk-Hydro Oil and Energy Company.

[7] Utsira – Demonstrating the hydrogen society on renewable terms. Norsk-Hydro Oil and Energy Company. Date: 4th December 2005

[8] A field application experience of integrating hydrogen technology with wind power in a remote island location, Robert Gordon University, Journal of Power Sources. Date: 18th January 2006.

[9] Island Wind-Hydrogen energy: A significant US Resource, Renewable Energy 33. Authors: Benjamin Sovacool & Richard Hirsh. Date: 4th December 2007

[10] Wind & Hydrogen Lolland community testing facilities, Renew Europe 2007 Hamburg. Senior Advisor Jesper Krogh Jensen. Date: 22nd March 2007

[11] Hydrogen and Renewables Integration (HARI), CREST (Centre for Renewable Energy Technology) Loughborough University. Authors: Rupert Gammon et al. Date: March 2006.

[12] James Blyth – Britain's first modern wind power pioneer, Wind Engineering Volume 29. Author: Trevor J. Price. Date: May 2005

[13] General Introduction to Wind Turbines. Website available from: www.earthscan.co.uk/Portals/0/Files/Sample%20Chapters/9781844074389.pdf. Date: September 2009

[14] Handbook of Wind Energy. Author: Tony Burton. Date January 2001. Page 4

[15] Energy Systems & the Environment, Course notes on Energy Resources and Policy (Betz Formula). Author: Dr Andy Grant. Date: 2009

[16] Wind Energy: Renewable Energy and the Environment, Authors: Vaughn Nelson and Abbas Ghassemi. Page 138-142. Date: 2009

[17] Wind Power Integration: connection and system operational aspects. Author: Brendan Fox. Date 2007, Pages 73-79.

[18] Fuel Cell Systems Explained. Authors: James Larminie and Andrew Dicks. Date Published: 2003.

[19] UHI Renewable Energy Course Notes, Hydrogen Fuel Cells (Image taken from Ballard Power Systems, www.ballard.com). Author: Alasdair Macleod

[20] A report on electrolysers, future markets and the prospects for ITM Power Ltd's electrolyser technology. Author: Professor Marcus Newborough. Date: February 2004.

[21] Summary of Electrolytic Hydrogen Production, National Renewable Energy Laboratory. Author: Johanna Ivy. Date: September 2004.

[22] A probabilistic method for sizing of isolated wind-electrolyser systems, Norwegian University of Science and Technology. Authors: Lars Nesje Grimsmo et al. Date: 2004

[23] Ground Source Heat Pumps and Applications, Renewable and Sustainable Energy Reviews. Author: Abdeen Mustafa Omer. Date: 28th July 2006

[24] Hydrogen Fuel Cell Engines, Hydrogen Properties. Available from: (website, www1.eere.energy.gov) pdf. Date: December 2001.

[25] US Department of Energy, Energy Efficiency and Renewable Energy, Hydrogen Storage. Available from: (website www1.eere.energy.gov). Date: 18th September 2008

[26] Hydrogen Cars Now, Liquid Hydrogen. Available from: (website www.hydrogencarsnow.com). Date: Viewed September 2009.

[27] Wind Hydrogen Production for Domestic Hydrogen Production?, University of the Highlands and Islands (Lews Castle College). Author: Dr Alisdair Macleod. Date: 2008

[28] Carbon Savings and Wind Power on Lewis, Views of Scotland Briefing, Paper 6. Date: October 2007.

[29] The Carbon Trust: Marine Energy Challenge, Oscillating Water Column Wave Energy Converter Evaluation Report. Date: 2005

[30] Isle of Lewis – Proposed Wind farm development areas (image), Website available from: http://www.jmt.org/assets/news/lewis_wind_map_fullw.jpg. Date: September 2009

[31] Lewis Wind Power, Website available from: http://www.lewiswind.com/projectcentre/. Date: September 2009.

[32] Demand Side Management, Towards a Carbon Neutral Community. Authors: Fairuz Abd Jamil et al. Available from website: http://www.esru.strath.ac.uk/EandE/Web_sites/06-07/Carbon_neutral/START%20PAGE.htm Date: June 2007

[33] Thermal Performances of Hot Water Heater in Series, University of Petroleum and Minerals, Dhahran, Saudi Arabia. Authors: A. K. Kar and K. M. Al-Dossary. Date: 1995.

[34] Legionnaire's Disease, Health & Safety Executive. Website available from: http://www.hse.gov.uk/legionnaires/ . Date: September 2009.

[35] Map of the Proposed area for wind-hydrogen project, Google Maps. Available from website: http://maps.google.co.uk/maps?hl=en&tab=wl . Date: September 2009.

[36] Bridging the European Wind Energy Market and a Future Renewable Hydrogen-Inclusive Economy, European Commission & Institute for Energy. Authors: S. Shaw, S.D. Petevs. Date: 2006

[37] Wind Power Electronics: Achieving lower cost, higher efficiency, and superior reliability. Author: Darren Hammell. Date: 30th June 2004.

[38] Sustainable Energy Technologies – Fuel Cell Power Inverter Efficiency, Website available from http://www.encyclopedia.com/doc/1G1-71352644.html . Date: March 8 2001.

[39] On the Combined Effect of Wastewater Heat Recovery and Solar Domestic Hot Water Heating, Canadian Solar Buildings Conference. Authors: Michael Kummert et al. Date: August 20-24 2004.

[40] Wind Resource Utilising Hydrogen Buffering, System Costs. Available from website: www.esru.strath.ac.uk Date: May 2009